

Visualization and Visual Analysis of Ensemble Data: A Survey

Junpeng Wang, Subhashis Hazarika, Cheng Li, and Han-Wei Shen, *Member, IEEE*

Abstract—Over the last decade, ensemble visualization has witnessed a significant development due to the wide availability of ensemble data, and the increasing visualization needs from a variety of disciplines. From the data analysis point of view, it can be observed that many ensemble visualization works focus on the same facet of ensemble data, use similar data aggregation or uncertainty modeling methods. However, the lack of reflections on those essential commonalities and a systematic overview of those works prevents visualization researchers from effectively identifying new or unsolved problems and planning for further developments. In this paper, we take a holistic perspective and provide a survey of ensemble visualization. Specifically, we study ensemble visualization works in the recent decade, and categorize them from two perspectives: (1) their proposed visualization techniques; and (2) their involved analytic tasks. For the first perspective, we focus on elaborating how conventional visualization techniques (e.g., surface, volume visualization techniques) have been adapted to ensemble data; for the second perspective, we emphasize how analytic tasks (e.g., comparison, clustering) have been performed differently for ensemble data. From the study of ensemble visualization literature, we have also identified several research trends, as well as some future research opportunities.

Index Terms—Ensemble data, visualization and visual analysis, literature analysis, taxonomy.

1 INTRODUCTION AND MOTIVATION

SCIENTISTS from multiple disciplines often need to study complex real-world phenomena with sophisticated computer simulation models, which are usually affected by a set of model configurations (e.g., input parameter values, boundary/initial conditions, phenomenological models, etc.). A single run of the model with a specific configuration is usually not sufficient to understand the physical phenomena. Because of the inherent uncertainty, scientists often try to run the model with different configurations to generate multiple realizations of the same experiment. The output, which is a collection of spatio-temporal results, is often referred to as an *ensemble*. With the advancing data acquisition techniques and increasing necessities to precisely model various physical phenomena (e.g., disaster management, weather forecasting, etc.), more and more ensemble data are generated at an unprecedented rate [1], [2]. However, due to the complex nature of ensemble data (like multi-dimensionality, multi-valuedness), it is not a trivial problem for domain scientists to fully comprehend them.

Visualization plays the role of leading domain scientists towards a better and more intuitive understanding of their data. Over the last decade, a wealth of ensemble visualization techniques have been introduced and encouraging results have been reported. For example, numerous contour and curve related visualization techniques have been proposed to reveal the uncertainty in spatial features of ensemble data [3], [4], [5], [6], [7]. Probability distributions have been used extensively in ensemble visualization works to model the underlying uncertainty [2], [8], [9], [10], [11], [12],

[13]. Different types of time-series charts and comparative visualization methods have been adopted to capture temporal trends of ensemble data [14], [15], [16], [17], [18], [19]. To effectively demonstrate different facets of ensemble data, coordinated multiple views are often employed and they are linked together with intuitive interactions to facilitate users' exploration [20], [21], [22], [23], [24], [25].

With the ever-growing amount of ensemble visualization publications, it has become increasingly important to have a structured overview of the current state-of-the-art approaches. Such a structured view will help us in extracting the essential commonalities in these works and in turn, help us identify the current research trends and possible future directions. With this as the prime objective, in this work, we present a structured survey of the research performed in the field of ensemble visualization.

1.1 Survey Scope and Intended Audience

From a broader point of view, ensemble data is a subset of uncertain data [26], [27], [28], where the uncertainty is introduced because of the multiple instances of the same physical quantity. This type of data can be generated in many different ways (and from many different disciplines).

In this work, we are specifically focusing on ensemble data generated from computer simulation models (as shown in Figure 1). Other than ensemble simulations, there are numerous different sources of ensemble data, such as biomedical image collections [29]; repeated trials of psychological experiments [30], collections of snort alerts and flows of network security data [31], etc. The reasons that we focus only on computer simulation ensembles in this survey are: (1) these ensembles have already covered a large enough body of literature, and they are the primary focus of domain scientists from numerous disciplines; (2) computer simulations are usually associated with a spatial field, and the

• J. Wang, S. Hazarika, C. Li and H.-W. Shen are with the Department of Computer Science and Engineering, The Ohio State University, Columbus, OH, 43210.

E-mail: {wang.7665, hazarika.3, li.4076, shen.94}@osu.edu

Manuscript received April 19, 2005; revised August 26, 2015.

presence of multiple values of the same physical property at each location of the field (generated via ensemble simulations) incorporates uncertainties of the simulations, thereby posing challenges to existing visualization techniques. For example, traditional volume rendering algorithm (for a deterministic spatial field) is not readily applicable, when it comes to visualizing multi-valued spatial fields generated by such ensemble simulations.

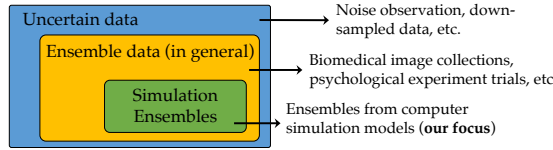


Fig. 1. This survey focuses on ensemble data from simulation models.

With computer simulation ensembles as the main focus, we analyzed papers in the past decade (year 2007~year 2017) from major visualization conferences (*IEEE Visualization Conference*, *Eurographics Conference on Visualization*, *IEEE Pacific Visualization Symposium*, *IEEE Large Data Analysis Visualization Symposium*) and journals (*IEEE Transactions on Visualization and Computer Graphics*, *Computer Graphics Forum*, *Computer Graphics & Applications*). Relevant earlier works that were referred in those papers have also been identified and included in our survey.

The intended audience of this survey are those who already have background in scientific visualization and possibly want to know more about uncertainty visualization, but have not had time to delve into ensemble visualization yet. As a result, we will not explain details about traditional visualization algorithms (like how volume rendering works), but focus more on demonstrating how traditional algorithms have been adapted to ensemble data. Our survey can also help existing ensemble visualization researchers to improve the understanding of their peers' works by providing a holistic overview of this field.

Difference with Existing Similar Works. From the visualization literature, we found four works that are similar to ours, i.e., [32], [33], [34], [35]. Our work distinguishes from them in the following aspects. First, we focus on a more specific group of ensemble data, i.e., computer simulation ensembles. Compared with the general survey of multi-faceted data by Kehrer and Hauser [34], our limited survey scope helps us categorize ensemble visualization works in a finer granularity and elaborate works in each category with sufficient details. Second, for the focused ensemble data, our survey is more comprehensive and covers more aspects of them. Compared with the short paper by Obermaier and Joy [35], our survey includes not only spatial aspect, but also other aspects, like temporal trend and parameter analysis, of ensemble data. Compared with the conceptual framework proposed by Kolesár et al. [32], our survey discusses not only the *comparison* task, but also other tasks, like *overview* and *clustering*, for ensemble data. Third, we focus more on elaborating how visualization techniques and analytic tasks have been adapted to or performed differently because of ensemble data. This limits the audiences of our work (to those who have certain knowledge about visualization) but also makes our work more ensemble specific. Lastly, com-

pared with the work of Love et al. [33] in 2005, which summarized three groups of ensemble visualization approaches (parametric, shape descriptor, and operator approach), our survey presents a more up-to-date view of this topic.

1.2 Survey Structure

Figure 2 shows the structure of this survey. The three second-level nodes represent the topics covered in Section 2, 3, and 4 respectively, in this paper.

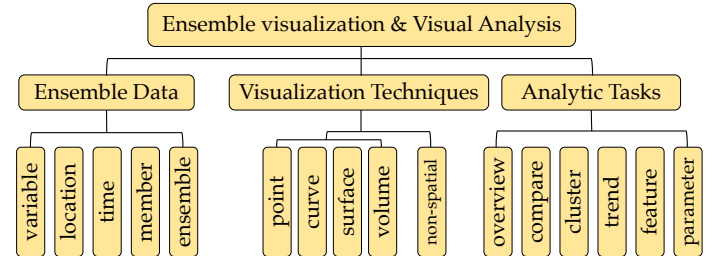


Fig. 2. The structure of this survey.

We start with the fundamental concepts of ensemble data by answering questions like: what is ensemble data; how ensemble data is different from traditional scientific data; and what makes the visualization of ensemble data difficult in **Section 2**. An intuitive data representation is formalized, which identifies the five orthogonal dimensions of ensemble data (i.e., *variable*, *location*, *time*, *member*, and *ensemble*). The representation is application independent, and thus, can be used to relate ensemble data from different disciplines.

Section 3 first partitions traditional visualization techniques based on whether a technique is for spatial data or not. This partition is similar to the differentiation between scientific visualization (SciVis) and information visualization (InfoVis) techniques, i.e., SciVis techniques focus more on data with spatial structures; whereas InfoVis techniques are more for the non-spatial representations of data. For SciVis techniques, we further partition them into *point-oriented*, *curve-oriented*, *surface-oriented*, and *volume-oriented* techniques, and discuss how traditional techniques (for deterministic spatial fields) in these four groups have been adapted to ensemble data individually. For InfoVis techniques, the research efforts focus more on how to combine them with SciVis techniques to present different facets of ensemble data in coordinated multiple views for visual analysis. These techniques often appear in integrated visual analytic systems developed under certain requirements from scientists. We summarize them into a separate subsection.

Ensemble visualization serves the general goal of uncertainty analysis, which, in practice, is usually accomplished by concrete low-level tasks. **Section 4** summarizes six common tasks we elicited from a structured analysis of existing literature, i.e., *overview*, *comparison*, *clustering*, *temporal trend analysis*, *feature extraction*, and *parameter data analysis*. Some of these tasks are unique for ensemble data, like the analysis of simulation parameters, whereas others are shared tasks when working with traditional deterministic data, like comparison and clustering. For the latter tasks, we focus more on elaborating how those tasks need to be performed differently to adapt to the analysis of ensemble data.

Our survey presents a structured review on the ensemble visualization literature, through which, we have identified several research trends and further visualization challenges. We have summarized them in Section 5.

2 ENSEMBLE DATA

Ensemble data (in the scope of our survey) is referred to as the data that contains a collection of outputs generated from computer simulation models. These outputs can either come from different executions of the same simulation model, ran with slightly different initial conditions or perturbed parameter settings (Monte-Carlo simulations [1]), or come from the executions of different simulation models themselves (multi-model simulations [23], [36], [37]). Each independent output in the collection is called as an ensemble *member* or a *realization* [38]. It is worth mentioning that members of the same ensemble may have some internal correlations or follow certain distributions, which are resulted from the generation process of those members (e.g. using statistical models for the perturbation of model parameters). In general, ensemble data is usually generated for one or multiple of the following purposes:

- model initial/boundary condition estimation or calibration [23], [39];
- parameter sensitivity investigation [25], [39], [40], [41];
- uncertainty quantification/mitigation [40], [42], [43];
- model comparison or model deficiency studies [23], [37].

With the significant advancements in data acquisition and momentous improvements in computing power, this type of data is generated at an unprecedented rate [1], [2], and from increasingly diverse disciplines. Table 1 lists some disciplines along with relevant ensemble visualization works.

TABLE 1
Disciplines and application areas that generate ensemble data.

Disciplines & Application Areas	Visualization Works
Meteorology and Climatology	[1], [23], [40], [43], [44], [45]
Astrophysics and High-Energy Physics	[17], [46], [47]
Oceanography	[20], [48]
Material Science	[49]
Hurricane/Hydrogeology	[50], [51], [52]
Automotive Engineering	[22], [53], [54]
CFD Simulations	[49], [51]

The major attribute that distinguishes ensemble data from traditional deterministic scientific data is their extra ensemble *member* dimension. On the one hand, ensemble data can have all the features that a deterministic scientific dataset has, such as multi-variate, multi-dimensional, spatio-temporal, etc. On the other hand, the individual members of ensemble data add a new dimension to the data. In other words, an ensemble data can be considered as multiple copies of a traditional scientific data, where each copy (each member) is a little different from the others.

2.1 Data Representation

To identify the structural and logical patterns in ensemble data, we formalize their data representation in this section. The representation also helps us organize publications

according to the features of the ensemble data in those publications.

For a typical execution of a computer simulation model, domain scientists need to set values for a set of N simulation parameters, denoted as:

$$P = \{p_1, p_2, \dots, p_N\} \quad (1)$$

where each parameter $p_i \in P$ has a range of interest $[ri_i^s, ri_i^e] \subset \mathbb{R}$, predefined based on the physical interpretation of the parameter. A sample from this N -dimensional parameter space is a parameter vector $\bar{x}_i \in \mathbb{R}^N$, i.e.,

$$\bar{x}_i = (x_1, x_2, \dots, x_N). \quad (2)$$

The simulation model, denoted as S , takes this parameter vector as input and generates a temporal sequence $S(\bar{x}_i)$ (an ensemble member m_i), which consists of T time steps, i.e.,

$$S(\bar{x}_i) = m_i = \{f_1, f_2, \dots, f_T\} \quad (3)$$

where f_i is the simulation field for the corresponding time step. For some simulations, the f_i for different time steps are the same, whereas others may have time-varying fields.

Each field f_i is composed of numerous observation points (locations, see Equation 4). Depending on the simulation settings, these locations may be organized as a regular grid (e.g., Cartesian grid, curvilinear grid [40], cylindrical grid [55], etc.) or an irregular point cloud [56].

$$f_i = \{l_1, l_2, \dots, l_L\}. \quad (4)$$

Each location l_i stores the simulated results for multiple scalar/vector variables (e.g. temperature, velocity). The set of variables, V , at each location, l_i , can then be denoted as:

$$V_{l_i} = \{v_1, v_2, \dots, v_V\}. \quad (5)$$

Ensemble simulations consist of multiple such executions, each uses a different parameter sample \bar{x}_i , or a different simulation model. The difference in \bar{x}_i , or the simulation models, leads to the difference in the resulting ensemble members. In the semantic example shown in Figure 3 (top), the ensemble data contains M members; each member has T time steps; the spatial simulation field of each time step has 16 locations (organized as a 4×4 Cartesian grid); each location (shown as a red dot) records multiple variables.

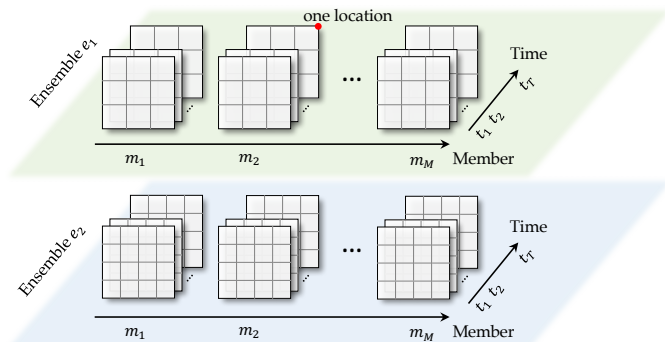


Fig. 3. The five dimensions of ensemble data. This semantic data has two ensembles of different spatial resolutions, e_1 and e_2 ; each ensemble has M members; each member has T time steps; the simulation field at each time step has 16/25 locations for the first/second ensemble; each location (the red dot) records values for multiple variables.

Additionally, we found that domain scientists may need to study multiple ensembles at the same time. These ensembles are usually closely related, but with difference in a crucial simulation configuration. For example, to capture different scales of the interested physical phenomena, meteorologists perform weather simulations (using the Weather Research and Forecasting model, i.e., WRF) in the same physical region with different spatial resolutions [25]. By comparing the resulting ensembles, they can investigate how different spatial resolutions affect the sensitivity of input parameters, the time complexity of executions, the accuracy of simulation outputs, etc. They can also get better ideas on balancing the computational cost and simulation accuracy [40]. The semantic example in Figure 3 shows two ensembles with different spatial resolutions (one with 4×4 and one with 5×5 Cartesian grid). It is worth mentioning that different ensembles usually use different sets of simulation parameters, and the numbers of members in different ensembles are not necessarily the same [25], [40].

From the above analysis, we identify five orthogonal dimensions of ensemble data, i.e., **variable**, **location**, **time**, **member**, and **ensemble**. We extend this analysis to ensemble data from all the papers we surveyed, and find that these five dimensions can cover the space of ensemble data very well. We, therefore, organize papers based on the existence of these five dimensions in the ensemble data studied in those papers (the "Ensemble Data" column in Table 3). The existence of one dimension means the size of that dimension is larger than one. For example, a time-varying ensemble has the *time* dimension, as it contains multiple time steps; however, the *time* dimension does not exist in any static ensembles, as the number of time steps is only one for them.

The five dimensions also lead to five features of ensemble data, i.e., multi-variate (resulted from the *variable* dimension), multi-dimensional [33] and spatio-temporal [16], [19] (resulted from the *location*, *time* dimension), multi-valued [57] (resulted from the *member* dimension), and multi-resolution [40] (resulted from the *ensemble* dimension), which makes ensemble data usually large and complex. Assuming the number of variables, observation points, time steps, members, and ensembles (in different resolutions) is v , l , t , m , and e respectively, the space-complexity of the ensemble data will be in the order of $\mathcal{O}(v \cdot l \cdot t \cdot m \cdot e)$. All the five numbers can be very large. Consequently, the size of ensemble data can easily reach tera- or petascale [57]. Analyzing this type of data and providing insights into the relationship among variables, uncertainty in feature properties, temporal evolution trend, variance among different members or among different ensembles are not trivial.

Parameter data and ground-truth data. Two additional types of data often come together with ensemble data. The first type is the input settings of simulation models, which can be boundary conditions, model configurations, parameter settings, etc. We call all these possible input settings as *parameter data* in this work. Building connections between input parameters and output ensembles is one of the most important analytic tasks for ensemble visualization. The second type is the *ground-truth data*. For example, the observed weather condition from satellites can be the ground-truth for WRF ensembles [25], [40]. Ground-truth data are often used to assess the quality of ensemble members or calibrate

model parameters [39]. Parameter data (simulation inputs) are always associated with ensemble data (simulation outputs), though they may not be the focus of analysis in certain cases. However, the existence of ground-truth data is highly dependent on the domain problems.

2.2 Emerging Visualization Problems

After the formal definition and comprehensive explanation on ensemble data, we would like to point out two emerging problems because of which traditional visualization techniques cannot be directly applied to ensemble data.

Additional dimension. Ensemble data introduces a new data dimension, i.e., the *member* dimension, which is usually not covered by traditional visualization techniques. For example, the direct volume rendering algorithm can render a single-valued scalar field volume; but it falls short of rendering a multi-valued volume (each grid point has multiple scalar values), because sampling and interpolation in the multi-valued field are not well defined [58]. A straightforward adaption of this algorithm to ensemble data is to aggregate the collection of values at each grid point to a single value before visualization, e.g., volume rendering of the mean volume. However, the adaption is not always appropriate. For example, visualizing the mean volume is misleading if the underlying ensemble members (collection of values at each grid point) follow a bi-modal or multi-modal distribution.

Multiple facets. The five dimensions of ensemble data make them multi-faceted [34], and domain scientists often need to investigate these facets simultaneously. However, a single visualization technique can only cover one or two of the five dimensions. For example, a parallel coordinates plot can cover *member* and *variable* dimensions of ensemble data, if using one parallel axis for one variable and one polyline for one ensemble member. However, the spatio-temporal facet of each member cannot be demonstrated at the same time. Integrated visual analytic systems (developed under specific requirements from domain scientists) are often in need. These systems (like Ovis [20], Noodles [43]) with multiple coordinated views and user-friendly interactions have successfully helped to address real-world problems of ensemble data from domain scientists.

Our survey reviews how traditional visualization techniques have been adapted to handle the *extra dimension* of ensemble data (Section 3), and how different analytic tasks have been performed to demonstrate and connect the *multiple facets* of ensemble data (Section 4).

3 VISUALIZATION TECHNIQUES

Computer simulation ensembles are usually embedded in a concrete spatial field/domain, and visualizing the spatial field is one of the fundamental requirements of domain scientists. Therefore, we classify visualization techniques for spatial data into four categories based on their focused geometric features, i.e., *point-oriented*, *curve-oriented*, *surface-oriented*, and *volume-oriented*.

Due to the extra *member* dimension, traditional visualization techniques in those four categories usually cannot be directly applied to ensemble data. Ensemble visualization

techniques usually resort to statistical aggregation (before visualization), visual composition (after visualization), or the combination of both to handle the extra *member* dimension. Following this, a very general ensemble visualization pipeline can be elicited, as shown in Figure 4.

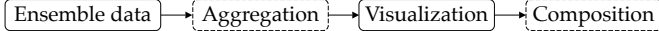


Fig. 4. A general visualization pipeline. Ensemble data will go through: a statistical aggregation step before visualization, or a visual composition step after visualization, or the combination of both steps. The *aggregation* and *composition* steps are in rectangles with dashed line borders, indicating they may not always appear in all pathways of this pipeline.

The *aggregation* step uses statistical summaries to aggregate the *member* dimension. Visualizations can then be applied on the resulting summaries to reveal the collective patterns/behaviors of the ensemble data. Examples of the statistical summaries include: calculating mean, variance, order statistics of ensemble members [6], [7], modeling probability distributions of ensemble members [8], [12], clustering ensemble members [4], [5], etc. Note that, the statistical aggregation may be applied on the physical quantities from different members (e.g. computing the mean of temperature values recorded in different members) or the geometric features extracted from them. For example, the ensemble members may be represented as iso-surfaces or curves (either directly outputted from ensemble simulations or generated from a pre-processing step). The aggregation of them (e.g. averaging iso-surfaces, clustering curves) usually needs more sophisticated algorithms. The *composition* step, which handles the member dimension after visualizations, composites the visualizations of individual members (or the visualizations of different statistical summaries [59]) to reveal the collective behaviors of the ensemble data. Typical visual composition approaches include: superimposition, juxtaposition, nesting, and overloading, as surveyed by Javed and Elmquist [60]. We discuss how the four categories of traditional visualization techniques have been adapted to ensemble data, in Section 3.1, 3.2, 3.3, and 3.4, according to different pathways in this general pipeline (e.g. aggregation before visualization, composition after visualization).

Computer simulation ensembles can also be aggregated/abstracted into non-spatial data for the overview of them. Different kinds of non-spatial visualization techniques have been used, together with spatial visualization techniques, to visualize ensemble data with different levels of detail. We discuss these techniques in Section 3.5.

3.1 Point-Oriented Techniques

The point-oriented visualization techniques map data at each grid point (of the spatial field) to selected visual channels. Examples of point-oriented techniques for deterministic scientific data include pseudo-coloring (mapping values to colors) and glyph visualization [61] (mapping values to shapes). Figure 5 shows an example of glyph visualization. On the left, the size of a sphere encodes the scalar value at the corresponding location; on the right, the size/direction of an arrow encodes the magnitude/direction of a vector.

For ensemble data, each grid point has multiple scalar or vector values, and a desired visualization should be able

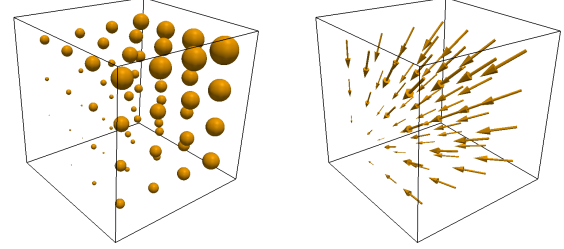


Fig. 5. Glyph visualizations. Left: using the size of spheres to encode the scalar value at each grid point; right: using the size/direction of arrows to encode the magnitude/direction of vectors at each grid point.

to effectively demonstrate the collective patterns of those values. Following the general pipeline in Figure 4, the point-oriented techniques have been adapted to ensemble data by: (1) aggregating the multiple values at each grid point, and visualizing the aggregated results with traditional methods; (2) visualizing individual values first, and then compositing their visualizations at each grid point.

3.1.1 Aggregation before Visualization

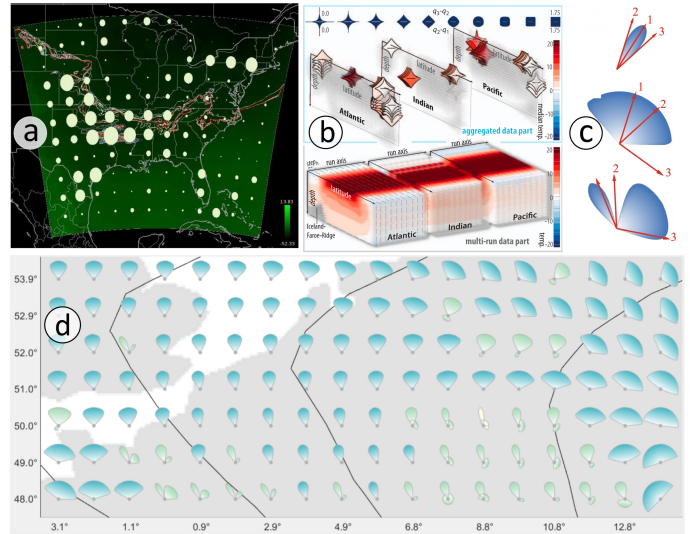


Fig. 6. Aggregation before visualization: (a) using circular glyphs to show the 95% confidence interval at each grid point, image courtesy of Sanyal et al. [43] © 2010 IEEE. (b) The color, size, upper/lower shape of superellipse glyphs encode the median, interquartile range, and sub-quartile range of all members, image courtesy of Kehrer et al. [62] © 2011 IEEE. (c) Using lobular glyphs to show the modality of vector directions at each grid point; (d) results of placing lobular glyphs across the simulation field. Image courtesy of Jarema et al. [63] © 2015 IEEE.

The first group of point-oriented visualization techniques aggregates the ensemble data at each grid point, and uses glyphs to depict the aggregated results. For example, Sanyal et al. [43] computed the 95% confidence interval of values at each grid point and mapped the interval to the size of circular glyphs (Figure 6a). Kehrer et al. [62] calculated the order statistics of ensemble members at each grid point and presented the statistics with superellipse glyphs (the glyph legends are shown in the top part of Figure 6b). The color, overall size, upper shape, and lower shape of each superellipse represent the median, interquartile range (i.e., $q_3 - q_1$), the range of $q_3 - q_2$, and the range of $q_2 - q_1$.

respectively (q_1 , q_2 , and q_3 represent 25%, 50%, and 75% of the ensemble values at each grid point).

For vector field ensembles, Jarema et al. [63] proposed lobular glyphs to encode the modality of vectors' direction at each grid point. As shown in Figure 6c, the topmost glyph represents a unimodal distribution of vectors' direction with a small variance; the middle glyph also represents a unimodal distribution, but with a larger variance; the bottom glyph represents a bi-modal distribution. Figure 6d shows the visualization results after placing the lobular glyphs across the entire simulation field.

The aggregated statistics can also be encoded into the positions of grid points (e.g., transferring grid points to a new space, where the points with a more similar collection of values are closer to each other [64]), the temporal behaviors of grid points (e.g., using flickers to encode variance [17]), etc. A complete set of examples can be found in Table 3.

3.1.2 Composition after Visualization

The second group of point-oriented visualization techniques visualizes each ensemble member first, then composites the visualizations of different members at the same grid point. For example, Sanyal et al. [43] proposed *graduated uncertainty glyphs*, where each member is visualized as a circular glyph first. The size of the circle represents the difference between the corresponding ensemble value and the mean value. Those circles (representing different members) at the same location were then overlaid/composited together to demonstrate the positional uncertainty, as shown in Figure 7a (smaller circles with darker colors are placed on top of bigger circles with lighter colors to avoid occlusions, i.e., circles are sorted based on their size). Figure 7b shows the result of using the *graduated uncertainty glyphs* to visualize the entire field. Hlawatsch et al. [51] proposed flow radar glyphs for uncertain flow fields. For their data, each grid point has a collection of time-varying vectors. They first visualized each time-varying vector (each member) as a curve-like glyph through a radial mapping (Figure 7c), then composited the curve-like glyphs from all members to derive a radar-shape glyph (Figure 7d). Figure 7e shows the results of placing the flow radar glyphs into different locations of the simulation field.

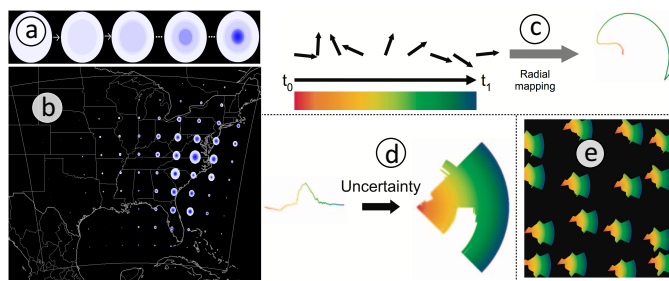


Fig. 7. Composition after visualization. (a) Graduated uncertainty glyphs: concentric circular glyphs representing individual members are sorted (based on their size) and overlaid together; (b) graduated uncertainty glyphs across the simulation field. Image courtesy of Sanyal et al. [43] © 2010 IEEE. (c) Flow radar glyphs: visualizing each time-varying vector through a radial mapping; (d) encoding member uncertainty through visual compositions; (e) applying flow radar glyphs to the simulation field. Image courtesy of Hlawatsch et al. [51] © 2011 IEEE.

3.2 Curve-Oriented Techniques

The curve-oriented visualization techniques extract and visualize curve-like features from the spatial simulation field. Traditional curve-oriented techniques include iso-contour visualization for 2D scalar field, streamline and pathline visualization for 2D/3D vector field. Given an iso-value of a deterministic scalar field (or a particle position of a deterministic vector field), a curve-like feature can be extracted with deterministic algorithms (e.g., level-set extraction methods, Runge-Kutta integration methods).

For ensemble data, an iso-value (a particle position) corresponds to multiple curve-like features (each from one ensemble member), and these features reflect the uncertainty encoded in the ensemble data. According to the general ensemble visualization pipeline (Figure 4), curve-oriented techniques have been adapted to ensemble data by: (1) aggregating curves with statistical summaries, and visualizing the resulted summaries; (2) visualizing individual curves (ensemble members) first, and then, compositing the curves to reveal the collective behavior.

3.2.1 Aggregation before Visualization

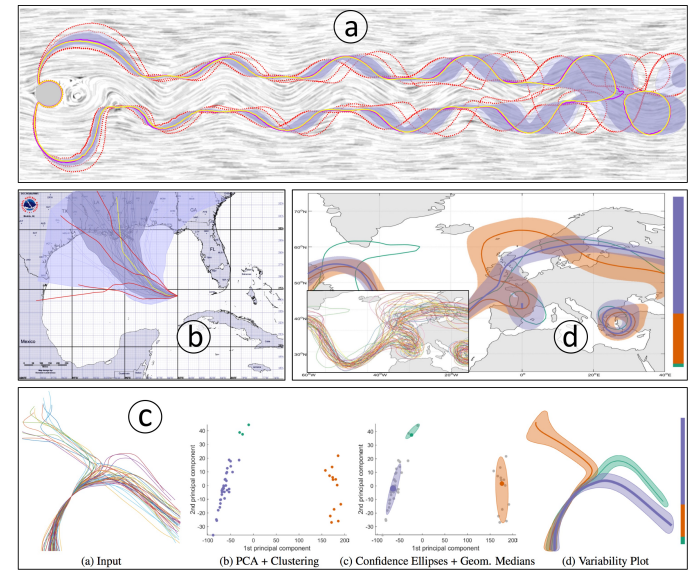


Fig. 8. Aggregation before visualization. (a) Contour boxplot: computing order statistics of ensemble curves and visualizing the statistics. Image courtesy of Whitaker et al. [7] © 2013 IEEE. (b) Curve boxplot: extending contour boxplot to streamlines/pathlines. Image courtesy of Mirzargar et al. [6] © 2014 IEEE. (c) Streamline variability plot: ensemble curves are first discretized into high-dimensional vectors; these vectors are then projected to 2D and clustered into three groups; mapping the geometric median and confidence ellipse of each group back to the curve space becomes a variability plot. Image courtesy of Ferstl et al. [5] © 2016 IEEE. (d) Extending the idea of streamline variability plot to contours. Image courtesy of Ferstl et al. [4] © 2016 John Wiley & Sons, Inc.

The first group of curve-oriented ensemble visualization techniques derives summary statistics (e.g., order statistics, probability distributions, clusters) of the curve-like features first, then encodes those statistics into visualizations. For example, the contour boxplot [7] derives the order statistics of curves based on the concept of data depth, and visualizes the median (the yellow curve in Figure 8a), 50% interval (the darker blue band), 100% interval (the lighter blue band),

and outliers (the dashed red curves), to demonstrate the ensemble of contours with uncertainty. Curve boxplot [6] extends the idea of contour boxplot to streamlines and pathlines. Figure 8b shows the visualization of a pathline ensemble (50 simulated hurricane tracks) using the curve boxplot. The same color scheme is used, except that the outliers are presented with red solid curves.

A curve-like feature can also be represented as a high-dimensional vector (by discretizing the curve into a sequence of disjointed points). Ferstl et al. proposed streamline variability plot [5], which projects ensemble curves (represented as high-dimensional vectors) as 2D points using PCA, and clusters them into different groups in the 2D space. They derived the geometric median and confidence ellipse for each cluster (statistical aggregation), and mapped them back to the original curve space for visualization. As shown in Figure 8c, the three clusters of ensemble curves are visualized with three bands/lobes (with color blue, orange, and green). The curve in the middle of each lobe and the shape of each lobe reflect the geometric median and confidence ellipse of each cluster in the 2D space respectively. The thickness of the median curve in each cluster also encodes the number of ensemble curves falling into that cluster. Extending the idea to contours, Ferstl et al. have also proposed contour variability plot [4], as shown in Figure 8d.

It is worth mentioning that some curve-oriented techniques for 2D scalar field are also applicable to (or have been extended to) 3D scalar field, like contour boxplot [65] and contour variability plot [4]. Therefore, those techniques belong to both curve-oriented (for 2D scalar field) and surface-oriented (for 3D scalar field) techniques. Details about how we categorized the works can be found in Table 3.

3.2.2 Composition after Visualization

The second group of curve-oriented ensemble visualization techniques visualizes each curve first, then composites curves (extracted from different ensemble members) together to visualize the entire ensemble. The spaghetti plot [3] is the most intuitive example for this group, as shown in Figure 9a (a spaghetti plot for an ensemble of 2D contours). Different colors can also be assigned to different curves to differentiate different ensemble members [23].

This group of techniques can demonstrate the ensemble data with very intuitive visualizations. However, when the number of ensemble members is large, the visualizations can easily get cluttered, and even misleading. For example, Figure 9a and 9b show two different ensembles with two spaghetti plots. Overall, it seems these two ensembles have very similar contour shapes and contour distributions, which is not the real case. Figure 9c and 9d visualize two individual members (in the form of color-mapped scalar fields) from the ensemble demonstrated in Figure 9a and 9b respectively. Data values from small to large are mapped to colors from blue, over white (equal to iso-value), to red. It is obvious that the contour shapes in Figure 9c and 9d are very different. The two spaghetti plots, which composite all contours in individual ensembles together, cannot reveal this difference. Pfaffelmoser and Westermann [66] addressed this problem by revealing the contour orientation (direction from sublevel set to superlevel set) and gradient

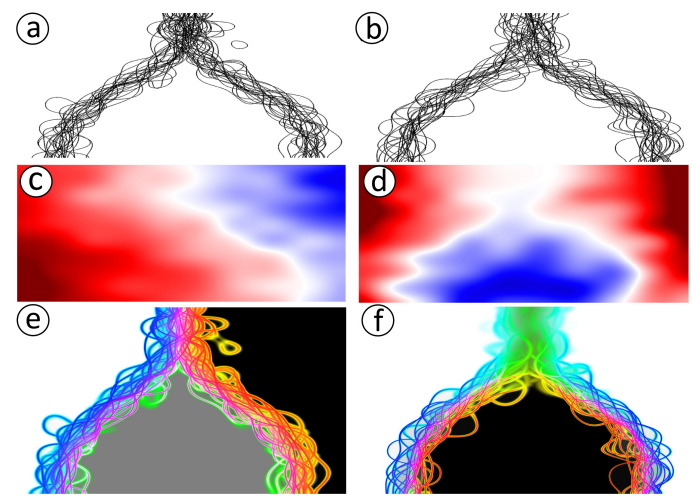


Fig. 9. Composition after visualization. (a, b) Two ensembles of contours are visualized with two spaghetti plots, the visualizations reveal little difference between the two ensembles; (c, d) one member from the ensemble (a), (b) respectively; data values from small to large are mapped to colors from blue, over white (equal to iso-value), to red; (e, f) Encoding contours' distribution and topology into spaghetti plot. Images are adapted from the work of Pfaffelmoser and Westermann [66] © 2013 The Eurographics Association.

distribution with three color schemes: one for the background and two for the foreground. The background color scheme (C_b : [white-gray-black]) indicates the orientation of the contours. For the regions in black (Figure 9e, 9f), all the members have values less than the iso-value; whereas, for the regions in white, all the members have values greater than the iso-value. The gray region highlights the spatial locations where a mix of members with values either greater or less than the iso-value. This color scheme effectively highlights the difference in contour orientations of similar looking spaghetti plots. The two foreground color schemes, C_l : [yellow-green-cyan] and C_u : [red-magenta-blue], indicate relatively low and high gradients along individual iso-contours. The presence of C_u indicates constantly large gradient magnitudes along the iso-contours, and no contrast between low and high gradient regions; while, the presence of C_l indicates a much lower gradient strength. The final spaghetti plot visualization (Figure 9e, 9f) can effectively differentiate the two ensembles with different curve orientations and gradient distributions.

3.3 Surface-Oriented Techniques

The surface-oriented visualization techniques extract the surface structure (e.g., iso-surface, stream surface) from a 3D scalar/vector field for visualization. Examples of traditional surface-oriented techniques include marching cubes, iso-surface volume renderings (based on the ray-casting algorithm), and stream surface visualizations [67].

For ensemble data, multiple surface structures (each from one ensemble member) exist at the same time, which makes the traditional surface extraction and visualization techniques not readily applicable. The key challenge for visualization is to handle the multiple surfaces simultaneously, and effectively reveal the underlying uncertainty in those surfaces. From our study of the visualization lit-

erature, surface-oriented techniques have been adapted to ensemble data by: (1) calculating surface statistics of the uncertain simulation field (e.g., surface crossing probability in each voxel), and visualizing the statistics with volume visualization techniques; (2) compositing surface visualization results from individual members, and addressing the resulted visual clutter or occlusion problem.

3.3.1 Aggregation before Visualization

The first group of surface-oriented ensemble visualization techniques performs statistical aggregations on the surfaces first, then visualizes the aggregated statistics of all surfaces. For example, Pöthkow and Hege [68] proposed *positional uncertainty of iso-contours*, which aggregates ensemble data into a probability field, and uses volume rendering to visualize the field. Each probability value in a voxel (of the probability field) is the Level Crossing Probability (LCP) value for the interested iso-surface (i.e., the probability that the iso-surface passing through that voxel). Specifically, they first modeled values of all ensemble members at each grid point as a Probability Density Function (PDF). The LCP value is computed by employing a Monte-Carlo based sampling strategy to generate multiple realizations/samples for each voxel. Of the generated samples, the number of times a cell (voxel configuration) suggests that the iso-surface passed through the cell constitutes the LCP value for that voxel. The resulted LCP volume, which shows the probability of the iso-surface passing through the field, can then be visualized using volume visualization techniques. Later, they further extended their work by adding the correlation between neighboring PDFs of the PDF volume and proposed *probabilistic marching cubes* [12], as shown in Figure 10a. The legend on the bottom-left shows the transfer function that maps LCP values (from 0 to 0.5) to visual channels (transparency and color).

Following this direction, more works that target to precisely model the uncertainty (i.e., the PDF) at each grid location have been proposed. Those works employ parametric [12], [68], non-parametric [69], and mixed (parametric and non-parametric [13]) distributions to model the positional uncertainty in varying ensemble datasets. Additionally, besides Monte-Carlo sampling, closed-form solutions to compute the probabilistic iso-surfaces from the distribution field (the PDF volume) have also been proposed [70], [71].

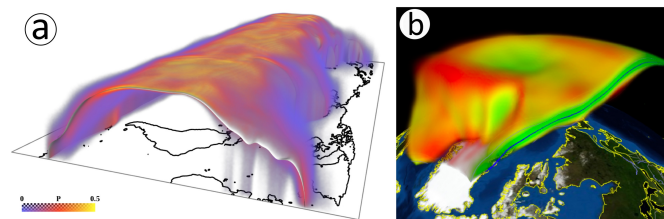


Fig. 10. Aggregation before visualization. (a) Probabilistic marching cubes visualize the level crossing probability volume of a specific iso-value using the direct volume rendering. Image courtesy of Pöthkow et al. [12] © 2011 John Wiley & Sons, Inc. (b) The volume rendering view of the iso-surface crossing probability, where the probability computation is integrated with the ray-casting algorithm. The iso-surface corresponds to a certain atmospheric temperature value and the distance to the mean surface is color-coded from green (low) to red (high). Image courtesy of Pfaffelmoser et al. [72] © 2011 John Wiley & Sons, Inc.

Another example for this group is the work of Pfaffelmoser et al. [72], as shown in Figure 10b. They proposed an alternative method of computing the first-crossing probability (i.e., the probability of crossing an iso-surface for the first time by a ray), which can be integrated into the ray-casting algorithm to visualize probabilistic iso-contours with spatial correlations. They introduced an incremental update scheme that allows efficient integration of the probability computation into the front-to-back volume ray-casting. For an effective visualization of the positional and geometrical uncertainty, they proposed a new color mapping scheme based on the approximated spatial deviation of possible surface points from the mean surface. Figure 10b shows their visualization of an uncertain iso-surface (of atmospheric temperature), where the distance to the mean surface (the blue curve) is color-coded from green (low) to red (high).

3.3.2 Composition after Visualization

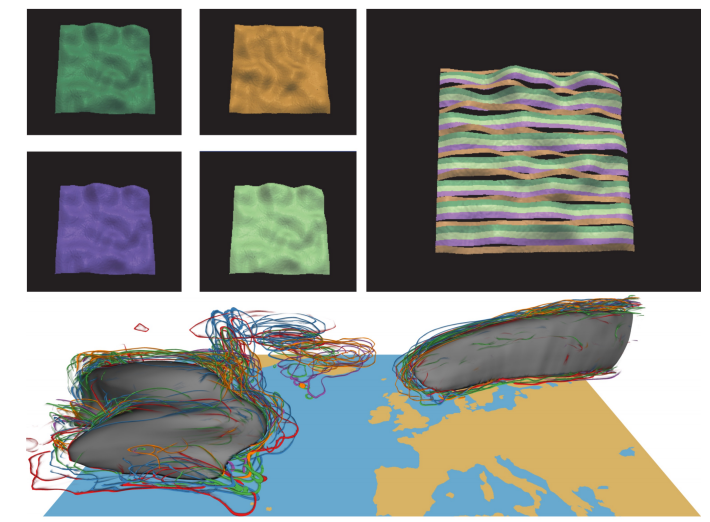


Fig. 11. Composition after visualization. Top: ensemble surface slicing, four ensemble surfaces are superimposed together. Users can quickly identify that the orange surface is different with the other three from the luminance discontinuity. Image courtesy of Alabi et al. [73] © 2012 SPIE. Bottom: screen-space silhouettes, the gray iso-surface represents the mean surface, ensemble members are visualized as silhouettes of iso-surfaces. Image courtesy of Demir et al. [74] © 2016 IEEE.

The second group of surface-oriented ensemble visualization techniques first visualizes individual ensemble members (as surfaces), then visually composites those members (surfaces) and addresses the potential occlusion problem. For example, Alabi et al. [73] proposed *ensemble surface slicing*, which cuts individual surfaces into multiple slices and organizes the slices from different ensemble members next to each other for members' structure comparison. As shown in Figure 11 (top), four ensemble surfaces (left) are composited together in one view (right: each is presented as a sequence of disjointed surface slices in the same color). From the luminance discontinuity in the composite visualization, one can easily identify that the orange member/surface is different from the other three. Another example for this group is the ensemble visualization work of Demir et al. [74] (i.e., screen space silhouettes). They visualized 3D surfaces (extracted from different ensemble members) using surfaces' silhouettes (in a certain viewing

direction) to alleviate the occlusion problem. Silhouettes for different surfaces are clustered (encoded with different colors), and composited together in the same 3D scene, as shown in Figure 11 (bottom). The gray surface shows the mean surface of all members, which works as a spatial context and visualizes the overall trend of all surfaces.

3.4 Volume-Oriented Techniques

The volume-oriented visualization techniques target to demonstrate a 3D simulation field, and reveal important inner structure of the field. Direct volume rendering is the most popular traditional volume visualization technique, which visualizes a 3D deterministic scalar field as a 2D image through the ray-casting algorithm.

An ensemble dataset usually has a multi-valued volume (it can also be considered as a collection of single-valued volumes), which makes traditional volume visualization techniques not directly applicable. Following the general pipeline, we observed that volume visualization techniques have been adapted to ensemble data by aggregating the multi-valued volume to a single-valued volume or a volume of PDFs, then applying traditional volume visualizations onto the aggregation results. A further composition step may also exist to composite separated visualization results.

3.4.1 Aggregation before Visualization

The first group of volume-oriented ensemble visualization techniques aggregates the multi-valued volume to a single-valued volume by aggregating the multiple instances at each grid point to a single instance. For example, assuming the ensemble members at each grid point follow a Gaussian distribution, the corresponding mean and standard deviation of values at each grid point can effectively represent the multi-valued volume. In other words, the ensemble of volumes can be aggregated to two volumes (one mean volume and one standard deviation volume). These two volumes can then be the input of the direct volume rendering. Djurcillov et al. [59] encoded the aggregated mean and uncertainty values (e.g., standard deviation or variance) into the color and transparency of their visualization through a 1D transfer function. As shown in Figure 12a, the white curve depicts uncertainty mapping (regions with higher uncertainty are less transparent); the color strip at the bottom shows the color mapping. Figure 12b and 12c show the visualization results for the variable “salinity” and “temperature” (of an ocean ensemble) respectively.

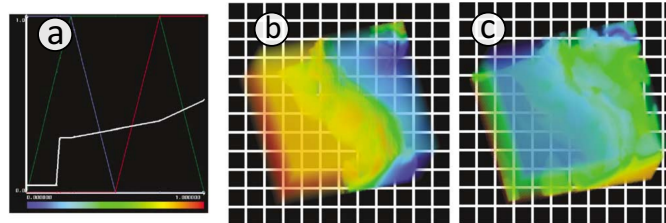


Fig. 12. Aggregation before visualization: (a) 1D transfer function that maps mean values to color and uncertainty values to transparency. (b, c) Volume rendering results of the *salinity* and *temperature* volumes. Image courtesy of Djurcillov et al. [59] © 2002 Elsevier Science Ltd.

3.4.2 Aggregation before, Composition after Visualization

The aggregated volumes, e.g., mean and uncertainty volumes, can also be rendered separately, and visualized together through a composition step. For example, Djurcillov et al. [59] visualized the mean and uncertainty of the ocean volumes through separate renderings. Figure 13a and 13b are the visualization results for the mean and uncertainty volume (the two images show the two volumes in the same viewing direction). The uncertainty volume was rendered as a gray scale image. They inverted the image’s pixel values and dithered the image into a gray scale bitmap. The dithering tried to distribute black dots (representing uncertainty) evenly into proper positions of the image, as shown in Figure 13c. The final visual composition step superimposed the volume rendering result of the mean volume (Figure 13a) and the uncertainty volume (gray scale bitmap, Figure 12c) to convey the uncertainty information along with the mean volume, as shown in Figure 13d.

Visualizing the mean volume is misleading in certain cases, as the underlying ensemble members may not follow a Gaussian distribution. Liu et al. [9] modeled the ensemble members at each grid point as a Gaussian Mixture Model (GMM). As a result, the original ensemble volumes became a single volume of GMMs. They could then sample the GMM volume to reconstruct a single-valued scalar volume, and use volume rendering to visualize it. Figure 13f, 13g, 13h, and 13i show the rendering results of their method using one, two, four, and six Gaussian components respectively, in comparison with the mean volume (Figure 13e). Repetitively sampling the GMM volume and visualizing the sampled single-valued volume, in a fixed viewing direction, can produce a sequence of rendering results (2D images). Playing these images frame by frame, as an animation, creates flicker effects in different image regions, and the frequency of the flickers reflects the uncertain level of those regions. The animation can be considered as the composition result of the sequence of 2D images, where the composition is conducted along the time dimension.

A more recent example in this category is the work of He et al. [75]. They modeled ensemble members at each grid point as a PDF, and binned the PDF evenly into separate value ranges. Each grid point then has a set of “range likelihood values” for the original collection of scalar values. For example, assuming the original ensemble has 100 members with scalar values ranging from 0 to 255, and the PDF at each grid point (modeled from the 100 values at that point) is divided into four even value ranges: range 1 (0-63), range 2 (64-127), range 3 (128-191), and range 4 (192-255). The original 100 volumes can then be aggregated into four range likelihood volumes, i.e., likelihood volumes for range 1, 2, 3, and 4. Each grid point of a range likelihood volume records the probability that its scalar value is in the corresponding range. He et al. then clustered the range likelihood volumes and built a range likelihood tree (shown in Figure 13j) of those volumes using hierarchical clustering. They could then explore the tree and render different range likelihood volumes (Figure 13k). The rendering results of different range likelihood volumes can also be composited (Figure 13l), using the multi-variate volume rendering (with a multi-variate Gaussian transfer function) [76].

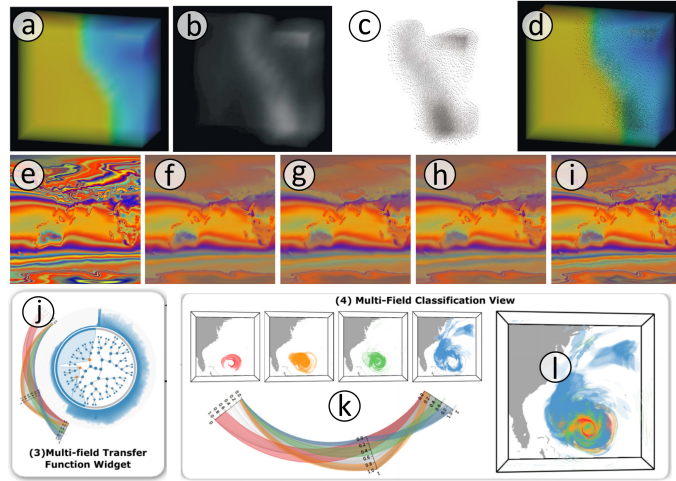


Fig. 13. Aggregation and Composition: (a, b) volume rendering result of the mean and uncertainty volume of an ocean ensemble; (c) inverting pixels' color of the uncertainty rendering result, and dithering it into a gray scale bitmap; (d) composition result of (a) and (c). Image courtesy of Djurcicov et al. [59] © 2002 Elsevier Science Ltd. Rendering result of an air temperature ensemble using the GMM based volume visualization: (e) mean volume visualization; (f-i) GMM volume visualization using one, two, four, and six Gaussian components. Image courtesy of Liu et al. [9] © 2012 IEEE. (j) Range likelihood tree of a hurricane dataset; (k) rendering results of different range likelihood volumes; (l) compositing rendering results of the four range likelihood volumes in (k) together. Image courtesy of He et al. [75] © 2017 IEEE.

3.5 Visualization Techniques for Non-Spatial Data

Visualization techniques for non-spatial data have also been used extensively in ensemble visualization. Most of those techniques can be easily adapted to ensemble data without any change. For example, Hazarika et al. [77] used a parallel coordinates plot to present the order statistics of ensemble surfaces. Wang et al. [25] adopted dendograms and heat maps to present an overview of member similarity in multi-resolution climate ensembles. Bock et al. [46] combined scatter plots and glyph visualizations to provide a global overview and comparison among members of a space weather ensemble. Demir et al. [78] employed line charts and bar charts (i.e., multi-charts) to demonstrate the value distribution across ensemble members.

The non-spatial visualization techniques are mostly for demonstrating different levels of abstraction/overview of the ensemble data, and they are often used along with multiple other spatial/non-spatial visualization techniques. These techniques together demonstrate different facets of ensemble data (with different levels of details) via different visualization views. With them together, as an integrated visual analytic system, domain scientists can perform specific visual analysis tasks and accomplish their analytical goals. We discuss the details of those tasks in Section 4.

4 ANALYTIC TASKS

The general goal of ensemble visualization is to depict the uncertainty encoded in ensemble data, from which useful information can be inferred. In practice, this general goal is usually accomplished by concrete visual analytic tasks. From the ensemble visualization works, we elicit six tasks,

which cover the major body of ensemble visualization literature. Note that, these tasks are not exclusively designed for ensemble visualization, and have been conducted in many other types of visualization works. In this survey, we focus on how they have been performed differently for ensemble data (i.e., how they cover the *member/ensemble* dimension). The six tasks are:

- 1) **Overview:** provide a concise visual summary of ensemble data and convey the overall uncertainty.
- 2) **Comparison:** visually identify the difference between two members or two ensembles of objects (e.g., two ensembles of values at two spatial locations) using juxtaposition, superimposition, and explicit encoding.
- 3) **Clustering:** divide members or ensembles of objects into separate groups, where similar members or ensembles are in the same group.
- 4) **Temporal Trend Analysis:** reveal how a single member, some members, or all members evolve over time.
- 5) **Feature Extraction:** extract geometric (e.g., vortex, eddy) or topological (e.g., source, saddle, sink point) features from the uncertain field of ensemble data.
- 6) **Parameter Analysis:** build connections between ensemble data and the simulation parameters.

These tasks appear to be the most popular ones with respect to ensemble visualizations, and they reflect the core interests and requirements of domain scientists. However, it is worth mentioning that they are not the complete set of tasks, and our intention is not to exhaust all possible tasks in this survey. Moreover, these tasks are not orthogonal to each other either. Some tasks may, to some extent, rely on others. For example, to build connections between ensemble data and simulation parameters, clustering ensemble data and parameter data separately and correlating the clusters from the two sides are often performed. Here, both the *clustering* and *parameter analysis* tasks are conducted, and the *parameter analysis* task relies on the *clustering* results.

4.1 Overview

Overview aims to present a high-level visual abstraction of the data. It is usually designed to be seen at the first glance before any interactions. Therefore, the overview is often presented as a static scene and provides informative hints for the following explorations.

For ensemble data, the overview task is to present all ensemble members and reveal the collective behavior (usually *the spatial or temporal behaviors*) of them. To make the visual representation concise, certain levels of abstractions may need to be applied to each ensemble member. For example, the box-plot based approaches (i.e., contour box-plot [7], curve box-plot [6] in Figure 8a, 8b) present an overview of a collection of curves/contours (i.e., members) by showing their order statistics. From the statistics, one can identify the major trend, the divergent scale, and the outliers of the entire ensemble. The time-series plots abstract/aggregate each ensemble member and present it as a line. Lines representing different members are then superimposed into a 2D time-line chart (one axis for time and the other axis for the interested quantity), to demonstrate the overall temporal trend of one ensemble [23], [46]. Those lines (representing individual members) can further be aggregated to avoid

visual clutters. For example, Potter et al. [23] demonstrated the temporal overview of their ensemble data with quantile trend charts (Figure 14a). The minimum and maximum bounds (blue curves) show the value range of the entire ensemble; the inter-quantile band (in gray) shows 50% of members ordered in the center of the ensemble; the median (black curve) shows the representative trend of all members.

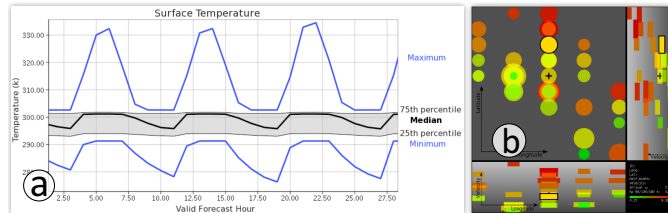


Fig. 14. (a) Quantile trend chart: computing the order statistics of lines representing different ensemble members in the time-line chart and visualizing their order statistics for ensemble overview. Image courtesy of Potter et al. [23] © 2009 IEEE. (b) Glyphs for parameter space overview: color and size represent the speed and opening angle (two parameters) respectively. The position of each glyph reflects the longitude, latitude values (another two parameters) for the corresponding ensemble member. Image courtesy of Bock et al. [46] © 2015 IEEE.

Except the aforementioned spatial or temporal overview, *overview of the parameter settings for all ensemble members* is also of paramount importance to domain scientists. For example, Bock et al. [46] encoded the four parameters (longitude, latitude, initial speed, and opening angle) associated with individual members (of a space weather ensemble) into circular glyphs, and presented the glyphs for all members in a 2D plot to overview the ensemble parameter settings. As shown in Figure 14b, the 2D plot is divided into three sub-views, which present three cuts of the parameter space. The top-left view shows the longitude and latitude coordinates of each member, whereas the bottom-left and top-right views show the speed along longitude and latitude directions. The color and size of each glyph encode the speed magnitude and opening angle of the corresponding ensemble member. From this overview of all parameter settings, users are allowed to select individual glyphs to further explore the corresponding ensemble members.

To some extent, most of the ensemble visualization works provide an overview of all ensemble members, as it is a very fundamental task. In the “Overview” column of Table 3, we use character S, T, and P (representing spatial, temporal, and parameter overview) to reflect what aspects of the overview task is focused on in individual works.

4.2 Comparison

Comparison, as a general visual analytics method, allows us to identify the similarities/dissimilarities between different data instances. Gleicher et al. [79] categorized comparative visualization techniques into three groups: superimposition, juxtaposition, and explicit encoding, through their analysis of the visualization literature. For ensemble visualization, this categorization is still applicable, but the subjects of comparison are not limited to only two data instances (e.g., two members/time steps), but also two collections of instances (e.g., two ensembles of values/curves) [80]. We

give examples (of ensemble visualization works) for both cases in the three categories of comparison techniques.

Juxtaposition puts multiple visualization results side-by-side for comparison. It relies on users’ short-term memory to identify the difference in the side-by-side views by frequently switching their visual attention between them. For example, Demir et al. [78] performed juxtaposed comparison in a 3D volumetric ensemble by putting individual volumes/members side-by-side for comparison. Selecting a specific value range of the volumes (using their multi-charts interface) will highlight different regions of those volumes. From the comparison, users can perceive how the value distributions are different in different 3D volumes (i.e., ensemble members). Höllt et al. [20] conducted juxtaposed comparison on two collections/ensembles of values at two different locations across time to reveal the uncertainty and uncertainty evolution at the two locations. As shown in Figure 15a, each vertical axis shows the comparison between the two locations (marked in the bottom right inset) at one time step. The two collections of values at the two locations are modeled as two PDFs, and put on two sides of the axis for juxtaposed comparison (the figure is further explained in Section 4.4 when we discuss the *temporal trend* task).

Superimposition aligns objects to be compared in the same context, which avoids implicit mental registrations of those objects to facilitate their comparisons. For example, Alabi et al. [73] superimposed four surfaces (as shown in Figure 11, top) to compare them in one view. The spatial alignment of the four surfaces helped Alabi et al. identify that the orange surface is different from the other three. Ferstl et al. [15] compared ensembles of curves and their cluster information, at different time steps, by superimposing them together, as shown in Figure 15b. The ensemble of curves (i.e., 2D iso-contours) at each time step are first visualized using a contour variability plot [4]. The plots for different time steps are then stacked together to show the curves’ cluster evolution over time. The superimposed comparison helps to track the ensemble of curves at different time steps.

Explicit Encoding quantifies the difference between the objects to be compared using specific metrics, and explicitly encodes the values of those metrics into visualization. For example, in the climate ensemble visualization work of Wang et al. [25], they computed the difference between the simulated precipitation value (from one member) and the observed precipitation value (from satellites) at all grid points of the simulation field, and mapped those difference values to different colors to assess the quality of the ensemble member. Köthür et al. [30] extended the use of Windowed Cross-Correlation (WCC) matrix to ensemble data to reveal the correlation difference between two time-varying ensembles. Conventionally, each cell of a WCC matrix stores the correlation between two windowed time segments from two different time-series (which can be two time-varying ensemble members). In the work of Köthür et al., each cell of their WCC matrix stores a collection of correlation values, which are the correlations (for the designated time segment) between all possible combinations of members from two different time-varying ensembles. Köthür et al. then designed glyphs for the cell to visualize the statistical summaries (e.g., mean, standard deviation, and quantile information) of those correlation values.

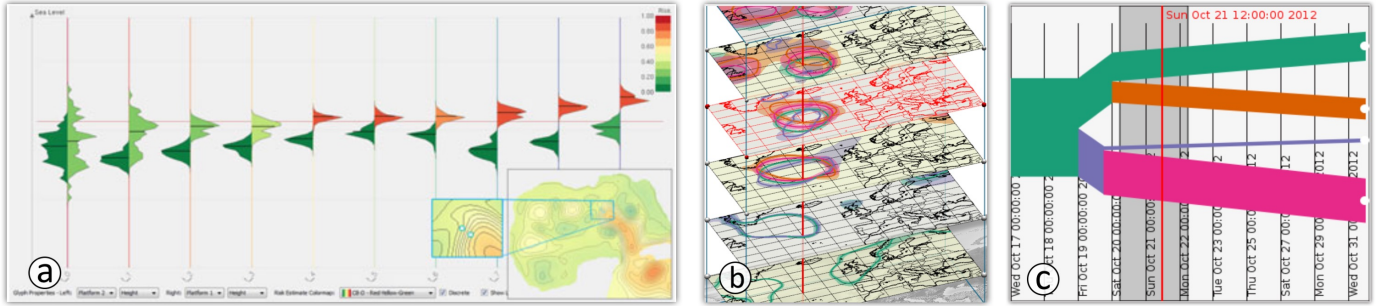


Fig. 15. Demonstrating temporal trend. (a) Visualizing and comparing the temporal trend at two points with violin plot glyphs. The horizontal/vertical axis of the chart is time/sea-level. At each timestamp, the PDFs of ensemble members at two points are shown as two violin plot glyphs side-by-side (for comparison). Image courtesy of Höllt et al. [20] © 2014 IEEE. (b) Temporal trend of ensemble curves with stacked contour variability plot; (c) parallel sets demonstrating the cluster splitting trend. Image courtesy of Ferstl et al. [15] © 2017 IEEE.

4.3 Clustering

Clustering divides data by putting data instances with similar features into the same group, which works as an effective way to reveal prominent data patterns. The commonly used clustering algorithms include: *k*-means [78], hierarchical clustering [25], DBSCAN [81], etc. For ensemble data, clustering can be used to cluster members or ensembles of objects (e.g., ensembles of values at different locations).

The difference in performing this task for ensemble data is in the use of new distance metrics for the clustering algorithms. For example, to cluster grid points of a deterministic simulation field (each grid point stores a single value), the distance metric can simply be the absolute difference between the values stored at those grid points. However, to cluster grid points of an uncertain field (each grid point stores a collection of values), new metrics that can measure the difference between collections of values have to be used. For example, we have seen ensemble visualization works that model the collection of values at each grid point as a PDF, and use the KL-divergence to quantify the difference between the PDFs in different locations [33].

From the ensemble visualization literature, we found that the distance metrics used in different ensemble visualization works (that contain *clustering*) are very different. Those metrics are very application-specific, and are significantly affected by data features. As the number of clustering related ensemble visualization works is not extremely large, we decided to present them all in this survey. Details about the used clustering algorithms, clustered objects, and applied distance metrics in those works are listed in Table 2.

Classification, which categorizes data instances into pre-defined categories [8], [92], is very similar to clustering (i.e., it also divides data instances into different groups based on their similarity). We, therefore, treat them equally with the *clustering* task in this paper. For ensemble data, the difference of classification lies in the way of generating the pre-defined categories. A typical classification example (of ensemble visualization works) is the work of Bensema et al. [8] (i.e., modality-driven classification). They modeled the collection of values at each grid point of an uncertain field (of their ensemble data) as a PDF. Grid points of the uncertain field are then categorized into four classes based on the modality of the corresponding PDFs: class-0 (grid points with a low variance value distribution), class-U (grid

points with a unimodal value distribution), class-B (grid points with a bi-modal value distribution), and class-M (grid points with a multi-modal value distribution). The classification result reveals the feature complexity (i.e., modality) encoded in the underlying ensemble members across different locations of the uncertain field. The ensemble-related classification works have also been summarized in Table 2.

4.4 Temporal Trend Analysis

The *temporal trend analysis* task is to capture how the data of interest evolve over time. It is a very important task in many domains, like weather predictions [25], [40], fluid dynamics simulations [18], and matter transitions in physics [17]. For ensemble data, the temporal trend needs to be extracted from either a single member (similar with the traditional temporal trend analysis), or a collection of members (the new part due to ensemble data). According to our study on the literature, temporal trends can be captured through three groups of approaches: (1) view compositions; (2) time-series plots and their variations; (3) pathline based visualizations.

View Compositions. To reveal temporal trends, the first group of visualization approaches relies on view compositions, i.e., juxtaposition or superimposition, to compare ensemble data at different time steps. *Juxtaposition* approaches demonstrate temporal information of ensemble data by putting visualization results of different time steps side-by-side for comparison. For example, in the climate ensemble visualization work of Wang et al. [25], they demonstrated 30 daily precipitations in 30 small-multiples (views), from which domain scientists can explore back and forth to perceive the temporal movement of precipitations over the region of interest. Animation can also be considered as a juxtaposition approach, as it also relies on users' short-term memory to build connections between time steps. The difference is that animation juxtaposes views along the time dimension, rather than a spatial dimension. For example, Hao et al. [17] employed animations in their ensemble visualization work to show the shape change of 3D spaces comprised of high-energy particles. *Superimposition* approaches overlay ensemble visualization results at different time steps together for direct comparisons. Although they can easily result in visual clutter, the superimposition approaches enable users to focus on one view and directly compare visualization results over time (need less efforts in mental

TABLE 2
Clustering (classification) algorithms and distance metrics used in ensemble visualization works.

Clustering Algorithm	Publication	Objects To Be Clustered/Classified	Distance Metric
<i>k</i> -means	Biswas et al. [40]	2D locations: each stores an ensemble of scalar values	The difference between derived <i>parameter sensitivity values</i> for different locations
	Demir et al. [78]	histograms: each describes the statistical summary of members in a spatial region	$\frac{1}{n} \sum_{i=1}^n (h_1(i) - h_2(i))^2$, where h_1, h_2 are two histograms and n is the number of bins.
	Splechtna et al. [82]	2D points: each represents a member with a pair of parameter values	Euclidean distance between the 2D points (the coordinates of each point are the corresponding member's parameter values)
	Kumpf et al. [83]	Members: each is represented as a collection of locations (a spatial region)	Euclidean distance between the linearized collection of locations (region of interest) from different members
<i>k</i> -medoids [84]	Potter et al. [85]	2D locations: each stores an ensemble of scalar values	using the scalar values (i.e., temperatures) as the feature vector for each location
DBSCAN [86]	Bruckner & Möller [14]	3D volumes: each is from a time step of an ensemble member	sum of squared intensity differences across all grid points (of different volumes)
	Liu et al. [81]	3D locations/voxels: each with a variation value derived from ensemble members (pathlines)	difference between the variation values (derived from the proposed <i>longest common subsequence</i>)
agglomerative hierarchical clustering (AHC)	Wang et al. [25]	Members: each is a time-varying 2D field	structure similarity (SSIM [87]) to quantify the difference between 2D fields, dynamic time warping (DTW [88]) to handle the time-varying feature
	Ferstl et al. [4], [5], [15]	Members: each is a streamline, pathline, or 2D/3D contour	Euclidean distance between points (representing the original streamlines/pathlines/contours) in the rank-reduced PCA space
	Hao et al. [17]	3D volumes: each is a spatial field for a temporal ensemble members	derived <i>shape dissimilarity metric</i> using Oc-Tree; use DTW to handle the temporal facet; Manhattan distance between temporal ensemble members
	Demir et al. [74]	Members: each is represented as a silhouette of the original 3D surface	$\sum_x (\sqrt{ f_i(x) - \mu } - \sqrt{ f_j(x) - \mu })^2 / m$, where x is a grid point, and f_i, f_j are two fields, μ is the iso-value and m is the number of grid point
	Jarema et al. [63]	Members: each is a 2D vector field	accumulating the similarity at each grid point, and normalizing by the number of points
	Bordoloi et al. [38]	(a) spatial ensemble members (realization); (b) locations with a collection of values	Manhattan distance $\sum_{i=1}^n p_i - q_i $: for (a), p_i and q_i are the i th wavelet coefficients of different members; for (b), p_i and q_i are the value of the i th member in different locations. They also discussed the use of KL divergence in case (b).
	He et al. [75]	3D volumes: each is a likelihood volume for a certain probability range	The likelihood volumes are linearized and normalized as PDFs. The distance used for clustering is the Jensen -Shannon divergence [89] between the PDFs.
<i>k</i> -means, AHC, and DBSCAN	Shu et al. [19]	2D locations: each stores an ensemble of time-varying values	difference between their derived <i>behavior vector</i> of each location
GMM approximation, AHC	Jarema et al. [21]	(a) particles: from different pathlines (members) at the same time step; (b) pathlines/members	Mahalanobis distance [90] on the modes derived from GMM approximations, (<i>transport similarity</i>)
nearest-neighbor-based density estimation [91], minimum spanning tree cluster analysis	Hummel et al. [49]	2D points: each is a point in the flow map	Euclidean distance between the end points, X' , in the flow map (flow map is a set of points resulted from tracing a set of particles X that start at time t and last over T , i.e., flow map $\phi(X, t, T) = X'$).
	Obermaier et al. [18]	p -dimensional points: each represents a feature extracted from members	Euclidean distance between p -dimensional points
correlation filtering, hierarchical cluster subdivision	Pfaffelmoser & Westermann [11]	2D locations: (of an uncertain field) each with a collection of scalar values	correlation strength (correlation neighborhoods and their cardinal numbers)
uncertainty projection	Chen et al. [64]	2D locations: each with a collection of scalar values	the difference between two collections of values, U_i and U_j , is defined as: $D(U_i, U_j) = \alpha E(\bar{U}_i, \bar{U}_j) + \beta J(U_i, U_j)$, E is the Euclidean distance between ensemble means, J is the Jensen -Shannon divergence, α, β are two adjustable parameters
PCA projection	Hazarika et al. [77]	3D locations: each with a collection of values (orders of each member)	the collections of values at different locations are considered as high-dimensional vectors and PCA is used to cluster them
modality-driven classification	Bensema et al. [8]	locations: of uncertain scalar fields	modality at each location (four types): identified using Hartigans' dip test on the collection of values at each location
error type based classification	Gosink et al. [92]	locations: of uncertain scalar fields	four types of error: identified based on statistical summary of values at each location

registration). For example, Ferstl et al. [15] stacked contour variability plots (2D visualization results) at different time steps together to create a space-time cube (Figure 15b), in which an overview on the evolution of iso-contours across time can be easily perceived. In general, the view composition approaches enable users to examine sufficient details about each time step. However, they usually do not scale well due to the limit of space or the visual clutter problem.

Time-Series Plots. Time-series (time-line) plots [20], [46] are effective in summarizing the temporal trends of ensemble data and demonstrating them as high-level abstractions. This type of 2D plot uses one axis to represent the time extension, and the other axis to demonstrate a statistical

measurement derived from ensemble data [19], [46]. Different ensemble members can be presented as curves overlaid in the 2D space, so that a direct comparison among members over time is available. Showing the cluster information of members at different time steps can also be accomplished in time-series plots by bundling curves of the same cluster into a strip [15], [21]. The resulting visualization is similar to parallel sets [93], which can effectively demonstrate the convergence/divergence of clusters over time. Figure 15c shows such a plot for the same ensemble data in Figure 15b. From this plot, it is very clear that the members are evolving into four clusters. Figure 15a is also an example of time-series plots for ensemble data. The horizontal axis is the

time dimension, and the value distributions of sea-level (one variable) at two locations are demonstrated along the vertical axis. The two collections of values (from all ensemble members at two locations) are modeled as two side-by-side PDFs. By comparing and tracking the pair of PDFs across time, one can observe that the temporal trend of the risk level at the two locations, represented by the left and right PDFs, are different. The left one always has low risk level, while the right one has an increasing risk level as its color changes from green (low risk) to red (high risk). Time-series plots usually can cover a long time range, but the temporal trends they presented are usually in high-level abstractions.

Pathline Demonstrations. For time-varying vector field ensemble data, pathlines are intuitive ways to show the underlying temporal trend with uncertainty. For example, Cox et al. [50] used a bunch of pathlines to show the predicted hurricane tracks. In their work, one pathline represents one possible trajectory of the hurricane (one ensemble member). Overlaying all pathlines from different members together shows the high/low probability regions that the hurricane will affect. When the *member* dimension is large, pathline based approaches can easily result in visual clutters. Therefore, instead of directly demonstrating pathlines, summary statistics of those pathlines are presented in certain scenarios. Uncertainty cones [42] and curve boxplots (when applied on pathlines) [6] are examples. Pathline based approaches are intuitive in demonstrating the temporal trend and uncertainty evolution, as they can be encoded directly into the simulation field. However, they are limited to vector field ensembles only, and cannot present details of ensemble members at a specific time step [52], due to the lack of synchronization among pathlines (at different time steps).

4.5 Feature Extraction

Feature extraction is to extract certain geometric/topological features of interest from a simulation field. Different from the four basic geometric features we discussed in Section 3, the features in this section are more sophisticated, such as flow transport behaviors (e.g., vortex, eddy), topological critical points (e.g., source, sink, saddle), etc.

For ensemble data, those features need to be extracted from an uncertain field. Their visualizations need to reveal not only the features themselves, but also the associated uncertainties. Here, we use an example of local vortex detections to elaborate how feature extractions have been extended to ensemble data. For a deterministic vector field, local vortex detectors compute a numerical criterion for each grid point (e.g., Q -criterion [94], λ_2 -criterion [95], etc.) and compare the criterion value with a user-specified threshold to decide if the grid point belongs to a vortex region or not. However, the numerical criterion cannot be directly computed from the uncertain field of an ensemble data. Otto et al. [10] addressed this problem using a Monte-Carlo approach. They first modeled the ensemble members at each grid point as a Gaussian distribution, with the consideration of spatial correlations between neighboring grid points. They then conducted Monte-Carlo sampling from the distribution, and computed the numerical criterion for each of the samples. As a result, each grid point would have a collection of criterion values. Comparing this collection of values with the user-specified threshold value, they

obtained a probability value for the grid point, indicating the likelihood that the grid point is in a vortex region. Doing this for all grid points, they derived a vortex probability field for the original uncertain vector field, which can be visualized using conventional iso-surface or volume visualization techniques. Figure 16a shows the iso-surface visualization of their vortex probability field with $P(\lambda_2 < -0.003)$.

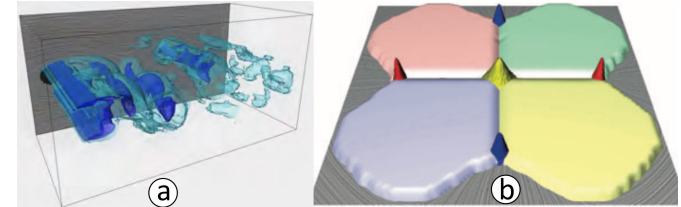


Fig. 16. (a) The Cylinder ensemble data set (time step 100): iso-surface visualization of the probability field $P(\lambda_2 < -0.003)$ with iso-values 0.05 and 0.95. Image courtesy of Otto et al. [10] © 2012 John Wiley & Sons, Inc. (b) LIC of v_c and uncertain critical points: the peaks in red/blue/yellow are source/sink/saddle points. Image courtesy of Otto et al. [96] © 2010 John Wiley & Sons, Inc.

Identifying critical points (i.e., source, sink, saddle) is an effective approach to analyze the topology of a spatial field. However, different from deterministic fields where the critical points have deterministic locations, the uncertain field of ensemble data brings challenges to critical points extractions. Targeting on this problem, Otto et al. [96], [97] generalized the concepts of streamlines to uncertain vector fields and proposed algorithms to identify critical points of the fields. In their work, they modeled the uncertain vector field as a density distribution function (i.e., the collection of vectors at each grid point was modeled as a Gaussian distribution) and performed streamline tracing on the function. Conventionally, for a specific integration step, the streamline tracing algorithm derives a deterministic location for a particle. For an uncertain field, the deterministic location becomes uncertain locations, and those locations constitute a particle density distribution at each integration step. Based on the derivative of the density distribution at different integration steps, Otto et al. extracted source, sink, and saddle points for the uncertain field. They also performed a Monte-Carlo approach to integrate probabilistic particle paths, so that they could segment the uncertain field. As shown in Figure 16b, the uncertain source, sink, and saddle points are represented as peaks (of a height field) in red, blue, and yellow. The regions in different colors show the segmented areas (affected by different source/sink points).

4.6 Parameter Analysis

The *parameter analysis* task is to build connections between parameter data and ensemble data, to analyze the uncertainty in simulation inputs. From domain scientists' perspective, the parameter data and ensemble data (simulation inputs, outputs) are closely related, and analysis should be conducted on both sides to build connections between them.

Sedlmair et al. [98] proposed a conceptual design framework for parameter analysis. Different with them, we only focus on parameter analysis works that related to ensemble data in this survey. Pure parameter analysis works, that have little connection with ensemble data, have been

excluded. The visualization of ensemble data has been thoroughly discussed in Section 3, we, therefore, focus on discussing how to visualize parameter data, and how to correlate the two types of data, in this section.

Visualizing Parameter Data. Considering a single parameter as a dimension, multiple parameters with different values (used in different runs) constitute a high-dimensional space. Therefore, parameter visualization can resort to high-dimensional data visualization techniques. According to our review, the most common approaches used for parameter visualization include Parallel Coordinates Plots (PCPs) [18], [24], [25], [44], wheel plots [99], scatterplots [22], [82], line charts [40], [82] and glyphs [46]. Most of those approaches not only present the parameter space, but also demonstrate the interrelations between different parameters. For example, a PCP can present each parameter with one parallel axis, and each parameter setting (for one run) with one polyline across all axes. The relational pattern formed between neighboring axes of the PCP can then demonstrate the correlation between the corresponding parameters.

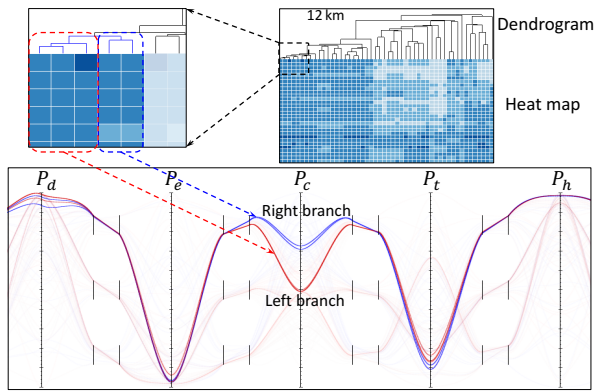


Fig. 17. Building connections between parameter data and ensemble data. Each column of the heat map represents one temporal ensemble member, and the members are clustered using hierarchical clustering. The difference between the two highlighted groups of members (in blue and red boxes) is resulted from the difference in the values of parameter P_c . Image courtesy of Wang et al. [25] © 2017 IEEE.

Connecting with Ensemble Data. There is a one-to-one correspondence between each instance of the parameter data (one parameter setting) and each ensemble member. Domain scientists usually study simulation parameters by exploring this correspondence to connect parameter data with ensemble data. Coordinated multiple views are usually employed to present parameter data and ensemble data simultaneously. Specifically, *brushing and linking* is the most commonly employed strategy to connect parameter views with ensemble views [40], [62]. Furthermore, we observed that finding the correspondence between clusters (i.e., clusters of parameter settings, clusters of ensemble members) is often more effective when correlating parameter data with ensemble data [14], [18]. In Figure 17, parameter data are presented in a variation of PCP, i.e., the nested PCP [25]; ensemble data are demonstrated with a linked visualization of a dendrogram (each leaf is an ensemble member) and a heat map (horizontal/vertical extension represents the *member/time* dimension). From the linked visualization, domain scientists can perceive how the value of P_c (one input parameter) is affecting the simulation outputs.

5 DISCUSSION

In the above two sections, we categorized visualization techniques into five categories, and summarized six analytic tasks of ensemble visualization. From the categorization and summarization, we found several research trends and some promising research directions, which are discussed in this section, along with the limitations of our work.

5.1 Observations, Research Trends

Uncertainty Modeling. Many visualization works analyze the uncertainty of ensemble data by modeling ensemble members as a PDF. We observed that visualization researchers devoted a lot of efforts in improving the accuracy of the PDF in reflecting the uncertainty. Those efforts are generally in two directions: (1) allowing more modalities; (2) considering the correlation among PDFs. With respect to the first direction, the Gaussian distribution was used extensively in ensemble visualizations to model a PDF. However, the underlying ensemble members may not follow a normal distribution [13]. To model the uncertainty in a better way, researchers have started looking into more complex models with higher modalities [8], [63]. This direction has also promoted the usage of non-parametric (e.g., kernel density estimations, histograms [2]) and semi-parametric (e.g., GMMs [9], [21]) models. For the second direction, researchers have started to consider the correlations between neighboring grid points [10], [116]. Scientific datasets often measure a continuous physical phenomenon with the inherent property of local data continuity. As a result, assuming the PDFs at individual grid locations to be independent might lead to incorrect modeling of uncertainty. [12] and [72] have studied this mis-representation and concluded that it is important to consider the spatial dependency among the PDFs at different grid locations. Consequently, the later batch of distribution based ensemble visualization works focus more on multi-variate distributions to better model uncertainties [12], [13], [69], [72].

Coordinated Multiple Views. We also observed that coordinated multiple views are used more often than a single static view in ensemble visualization works. In fact, it is rarely possible to demonstrate all facets of an ensemble in a single static view. The attempts will mostly result in information overload and/or visual clutter. Conversely, the different facets of ensemble data can be simultaneously demonstrated in coordinated multiple views, with different focuses in different views. Analyzing ensemble data will then require a process of exploration among those views, as well as interactions (e.g., brushing and linking) that drive the exploration. This observation/trend that visualizations are evolving from single static views to interactive visual analytic systems is not limited to ensemble visualization works, but also other types of visualization works.

5.2 Future Challenges and Opportunities

Ensemble visualization is still young [35], [57], and many works can be conducted for its advancements. We discuss several directions that we believe important and promising.

The Variable and Ensemble Dimensions. From our structured literature analysis, we found that the multi-variate feature (i.e., the *variable dimension*) of ensemble

TABLE 3

Ensemble visualization works are organized based on our discussions in Section 2, 3, and 4, i.e., ensemble data, visualization techniques, and analytic tasks. For the "Ensemble Data" column, cells with filled color indicate the size of the corresponding dimension is more than one. S/V in the "Variable" column represents scalar/vector variables. S/T/P in the "Overview" column represents spatial/temporal/parameter overview. J/S/E in the "Compare" column represents comparisons through juxtaposition/superimposition/explicit encoding. T/C/P in the "Trend" column represents time-series plot/view composition/pathline-based approaches. The footnotes of this table list works falling into the same category.

	Publications	Ensemble Member	Ensemble Time	Location	Variable	Point	Curve	Surface	Volume	Nonspatial Overview	Compare	Cluster	Trend	Feature	Parameter
Sanyal et al. [43]					S					S	J				
Chen et al. [64]					S					S	J				
Jarema et al. [63]					V					S	J				
Höllt et al. [20], [48]					S					ST	J		T		
Obermaier et al. [18]					V					T		T			
Gosink et al. [92]					S					S					
Günther et al. [100]					S					S					
Liu et al. [101]					V					S	J		C		
Jiao et al. [102]					V					SP	J				
Höllt et al. [103]					S					S	J				
Kehrer et al. [62]					S					S	J				
Bensema et al. [8] ¹					S					S					
Liu et al. [52]					V					S		C			
Hlawatsch et al. [51]					V					ST		C			
Pfaffelmoser et al. [104]					S					S					
Kao et al. [105] ²					S					S					
Sakhaee & Entezari [58]					S					S					
Ferstl et al. [4]					S					S					
Guo et al. [106]					V					S					
Pöthkow & Hege [69] ³					S					S					
Guo et al. [107]					V					ST	SE		TP		
Ferstl et al. [15]					S					ST	S		CT		
Jarema et al. [21]					V					S	J		TP		
Potter et al. [23]					S					ST	J		C		
Kumpf et al. [83]					S					S					
Liu et al. [108], [109]					V					S					
Hummel et al. [49]					V					S	E		P		
Fofonov et al. [16]					S					S	JS		T		
Ferstl et al. [5]					V					S			P		
Cox et al. [50]					V					ST			P		
Mirzargar et al. [6]					V					S			P		
Otto et al. [96] ⁴					V					S					
Whitaker et al. [7] ⁵					S					S					
Bürger et al. [110]					V					S					
Kern et al. [111]					V					S					
Thompson et al. [2]					S					S					
Hazarika et al. [77]					S					S	S				
Alabi et al. [73]					S					S	S				
Demir et al. [74]					S					S					
Pöthkow et al. [12] ⁶					S					S					
Bruckner & Möller [14]					S					ST	J		T		
Hao et al. [17]					S					S	J		C		
He et al. [75]					S					S	JS				
Demir et al. [78]					S					S	J				
Phadke et al. [47]					S					S	JS				
Bock et al. [46]					S					TP			T		
Liu et al. [81]					V					S			P		
Liu et al. [9] ⁷					S					S					
Biswas et al. [40]					S					ST	J		T		
Wang et al. [25]					S					TP	JSE		C		
Shu et al. [19]					S					ST	J		T		
Köthur et al. [30]					S					ST	E		T		
Poco et al. [112]					S					ST	JE		TC		
Malik et al. [113]					S					S	JE				
Piringer et al. [24]					S					P	J				
Splechtna et al. [82]					S					P					
Matković et al. [22] ⁸					S					P					
Matković et al. [54]					S					P					

¹ [11], [38], [85] ² [114] ³ [13], [70] ⁴ [10], [97], [115], [116] ⁵ [66] ⁶ [65], [68], [72] ⁷ [59] ⁸ [53], [117];

data has not been explored sufficiently. Although some works visualized multiple variables of ensemble data [22], [82], [117], analyzing the correlation or association between those variables was not their focus. Given that the variable correlation analysis is such an important topic of traditional scientific data, we believe it is also promising to explore it in the context of ensemble data, where the variable correlations will become uncertain correlations. Additionally, the *ensemble* dimension of ensemble data has not been covered by many existing visualization works either. Focusing on this dimension may lead to new research ideas and pioneering works. While it also depends on the availability of this type of data and specific requirements from domain scientists.

Expert Evaluation and Technique Portability. We also believe that more improvements can be conducted in the evaluation of ensemble visualization techniques. The effectiveness of a new technique is usually evaluated by domain scientists. However, several critical questions remain unanswered in making the evaluation rigorous. For example, how many domain scientists should participate in an evaluation to eliminate the subjective effects? How willing a domain scientist is to adopt a new technique? How much training time is required to get familiar with a new technique? Answers to these questions or a systematization on what aspects should be included in an evaluation will greatly improve the rigorouslyness of the evaluation. Additionally, how easily a proposed ensemble visualization technique can be applied to similar problems in other domains, i.e., the portability of the technique, is not well-discussed in most cases. Addressing this problem would significantly improve the reusability of ensemble visualization techniques.

Scalability. The scalability problem of ensemble visualization may consistently exist, since the attempts to simulate real-world physical phenomena are always intended to achieve higher spatial and/or temporal resolutions. Domain scientists' ambitions in generating more ensembles/members to better assess the underlying uncertainty of their models will also significantly increase the size of ensemble data. Therefore, concise data representations, well-organized memory structures, high performance data queries, and intelligent data movement strategies are always in need to support the increasing scale of ensemble visualization. From our review, we have seen multiple works that improve the performance of ensemble visualization through parallelizations, e.g., [81], [107]. The parallelizations can be conducted across different dimensions of ensemble data based on the specific analytic goals (e.g. parallelizing the computations across members, spatial locations, or time steps). In terms of data storage, most of the existing distribution based data reduction methods for uncertain data, e.g. [118], [119], can be used directly for ensemble data. However, using those methods is usually based on specific assumptions of the underlying member distributions, and certain modifications may need to be adopted to better preserve the features of ensemble data. Furthermore, we believe in-situ visualization [120] for ensemble data is also a promising direction in addressing the scalability challenge.

5.3 Limitations

As a structured analysis of literature, our work suffers from standard limitations associated with this type of works, i.e.,

the subjective nature of them. The perspectives we used to look at ensemble visualization papers, the criteria we used to select them, and the taxonomy we used to classify them are all affected by our way of understanding ensemble visualization. These subjective choices and decisions are by no means to be the best or unique. Equivalent analysis structures, taxonomies from different perspectives exist without any doubts. However, we also believe that our work is sufficient to provide a useful picture for the current research endeavors in ensemble visualization. Given that there are very few survey works for ensemble visualization, we hope our work can play as a starting point to meet the demanding need and lead to more comprehensive summaries or systematizations for this topic in the future.

Within the limited space, we focused more on summarizing the common features of different ensemble visualization techniques and validating the effectiveness of our proposed taxonomy. However, we believe our survey can be further extended by comparing the visualization works in the same category or across categories, e.g., discussing the merits and frailties of different techniques in different application scenarios. This would potentially lead to a conceptual design framework for ensemble visualization, and nourish more research on the theoretical analysis of this topic.

6 CONCLUSION

This paper presents a survey of ensemble visualization. The survey categorizes ensemble visualization techniques into five categories and reviews how traditional visualization techniques have been adapted to ensemble data. It also elaborates how six popular analytic tasks have been performed differently due to the unique features of ensemble data. With this survey, we connected the dots representing disparate ensemble visualization works and built up a big picture for this topic. We hope our work could help the theoretical analysis of ensemble visualization and support the development of novel ensemble visualization techniques.

ACKNOWLEDGMENTS

This work was supported in part by US Department of Energy Los Alamos National Laboratory contract 47145, UT-Battelle LLC contract 4000159447, NSF grants IIS-1250752, IIS-1065025, and US Department of Energy grants DE-SC0007444, DE-DC0012495, program manager Lucy Nowell.

REFERENCES

- [1] B. Hibbard, M. Böttinger, M. Schultz, and J. Biercamp, "Visualization in earth system science," *ACM SIGGRAPH Computer Graphics*, vol. 36, no. 4, pp. 5–9, 2002.
- [2] D. Thompson, J. A. Levine, J. C. Bennett, P.-T. Bremer, A. Gyulassy, V. Pasucci, and P. P. Pébay, "Analysis of large-scale scalar data using hexels," in *Large Data Analysis and Visualization (LDAV), 2011 IEEE Symposium on*. IEEE, 2011, pp. 23–30.
- [3] P. Diggle, P. Heagerty, K.-Y. Liang, and S. Zeger, *Analysis of longitudinal data*. Oxford University Press, 2002.
- [4] F. Ferstl, M. Kanzler, M. Rautenhaus, and R. Westermann, "Visual analysis of spatial variability and global correlations in ensembles of iso-contours," *Computer Graphics Forum (Proc. EuroVis)*, vol. 35, no. 3, pp. 221–230, 2016.
- [5] F. Ferstl, K. Bürger, and R. Westermann, "Streamline variability plots for characterizing the uncertainty in vector field ensembles," *IEEE transactions on visualization and computer graphics*, vol. 22, no. 1, pp. 767–776, 2016.

- [6] M. Mirzargar, R. T. Whitaker, and R. M. Kirby, "Curve boxplot: Generalization of boxplot for ensembles of curves," *IEEE Trans. on Vis. and Comp. Graphics*, vol. 20, no. 12, pp. 2654–2663, 2014.
- [7] R. T. Whitaker, M. Mirzargar, and R. M. Kirby, "Contour boxplots: A method for characterizing uncertainty in feature sets from simulation ensembles," *IEEE Transactions on Visualization and Computer Graphics*, vol. 19, no. 12, pp. 2713–2722, 2013.
- [8] K. Bensema, L. Gosink, H. Obermaier, and K. I. Joy, "Modality-driven classification and visualization of ensemble variance," *IEEE transactions on visualization and computer graphics*, vol. 22, no. 10, pp. 2289–2299, 2016.
- [9] S. Liu, J. A. Levine, P.-T. Bremer, and V. Pascucci, "Gaussian mixture model based volume visualization," in *Large Data Analysis and Visualization, 2012 IEEE Symposium on*, 2012, pp. 73–77.
- [10] M. Otto and H. Theisel, "Vortex analysis in uncertain vector fields," in *Computer Graphics Forum*, vol. 31, no. 3pt2, 2012, pp. 1035–1044.
- [11] T. Pfaffelmoser and R. Westermann, "Visualization of global correlation structures in uncertain 2d scalar fields," in *Computer Graphics Forum*, vol. 31, no. 3pt2, 2012, pp. 1025–1034.
- [12] K. Pöthkow, B. Weber, and H.-C. Hege, "Probabilistic marching cubes," in *Computer Graphics Forum*, vol. 30, no. 3, 2011, pp. 931–940.
- [13] S. Hazarika, A. Biswas, and H.-W. Shen, "Uncertainty visualization using copula-based analysis in mixed distribution models," *IEEE Transactions on Visualization and Computer Graphics*, vol. PP, no. 99, pp. 1–1, 2017.
- [14] S. Bruckner and T. Möller, "Result-driven exploration of simulation parameter spaces for visual effects design," *IEEE Trans. on Vis. and Comp. Graphics*, vol. 16, no. 6, pp. 1468–1476, 2010.
- [15] F. Ferstl, M. Kanzler, M. Rautenhaus, and R. Westermann, "Time-hierarchical clustering and visualization of weather forecast ensembles," *IEEE Transactions on Visualization and Computer Graphics*, vol. 23, no. 1, pp. 831–840, 2017.
- [16] A. Fofonov, V. Molchanov, and L. Linsen, "Visual analysis of multi-run spatio-temporal simulations using isocontour similarity for projected views," *IEEE transactions on visualization and computer graphics*, vol. 22, no. 8, pp. 2037–2050, 2016.
- [17] L. Hao, C. G. Healey, and S. A. Bass, "Effective visualization of temporal ensembles," *Visualization and Computer Graphics, IEEE Transactions on*, vol. 22, no. 1, pp. 787–796, 2016.
- [18] H. Obermaier, K. Bensema, and K. I. Joy, "Visual trends analysis in time-varying ensembles," *IEEE transactions on visualization and computer graphics*, vol. 22, no. 10, pp. 2331–2342, 2016.
- [19] Q. Shu, H. Guo, J. Liang, L. Che, J. Liu, and X. Yuan, "Enseblegraph: Interactive visual analysis of spatiotemporal behaviors in ensemble simulation data," in *2016 IEEE Pacific Visualization Symposium (PacificVis)*. IEEE, 2016, pp. 56–63.
- [20] T. Höllt, A. Magdy, P. Zhan, G. Chen, G. Gopalakrishnan, I. Hoteit, C. D. Hansen, and M. Hadwiger, "Ovis: A framework for visual analysis of ocean forecast ensembles," *IEEE Trans. on Vis. and Comp. Graphics*, vol. 20, no. 8, pp. 1114–1126, 2014.
- [21] M. Jarema, J. Kehrer, and R. Westermann, "Comparative visual analysis of transport variability in flow ensembles," *Journal of WSCG*, vol. 24, no. 1, pp. 25–34, 2016.
- [22] K. Matković, D. Gračanin, B. Klarin, and H. Hauser, "Interactive visual analysis of complex scientific data as families of data surfaces," *IEEE Transactions on Visualization and Computer Graphics*, vol. 15, no. 6, 2009.
- [23] K. Potter, A. Wilson, P.-T. Bremer, D. Williams, C. Doutriaux, V. Pascucci, and C. R. Johnson, "Ensemble-vis: A framework for the statistical visualization of ensemble data," in *2009 IEEE International Conference on Data Mining Workshops*, pp. 233–240.
- [24] H. Piringer, S. Pajer, W. Berger, and H. Teichmann, "Comparative visual analysis of 2d function ensembles," in *Computer Graphics Forum*, vol. 31, no. 3pt3, 2012, pp. 1195–1204.
- [25] J. Wang, X. Liu, H.-W. Shen, and G. Lin, "Multi-resolution climate ensemble parameter analysis with nested parallel coordinates plots," *IEEE Trans. on Vis. and Comp. Graphics*, vol. 23, no. 1, pp. 81–90, 2017.
- [26] G.-P. Bonneau, H.-C. Hege, C. R. Johnson, M. M. Oliveira, K. Potter, P. Rheingans, and T. Schultz, "Overview and state-of-the-art of uncertainty visualization," in *Scientific Visualization*. Springer, 2014, pp. 3–27.
- [27] C. R. Johnson and A. R. Sanderson, "A next step: Visualizing errors and uncertainty," *IEEE Computer Graphics and Applications*, vol. 23, no. 5, pp. 6–10, 2003.
- [28] A. T. Pang, C. M. Wittenbrink, and S. K. Lodha, "Approaches to uncertainty visualization," *The Visual Computer*, vol. 13, no. 8, pp. 370–390, 1997.
- [29] M. Hermann, A. C. Schunke, T. Schultz, and R. Klein, "Accurate interactive visualization of large deformations and variability in biomedical image ensembles," *IEEE transactions on visualization and computer graphics*, vol. 22, no. 1, pp. 708–717, 2016.
- [30] P. Köthur, C. Witt, M. Sips, N. Marwan, S. Schinkel, and D. Dransch, "Visual analytics for correlation-based comparison of time series ensembles," in *Computer Graphics Forum*, vol. 34, no. 3, 2015, pp. 411–420.
- [31] L. Hao, C. G. Healey, and S. E. Hutchinson, "Ensemble visualization for cyber situation awareness of network security data," in *Visualization for Cyber Security (VizSec), 2015 IEEE Symposium on*. IEEE, 2015, pp. 1–8.
- [32] I. Kolesár, S. Bruckner, I. Viola, and H. Hauser, "A fractional cartesian composition model for semi-spatial comparative visualization design," *IEEE Transactions on Visualization and Computer Graphics*, vol. 23, no. 1, pp. 851–860, 2017.
- [33] A. L. Love, A. Pang, and D. L. Kao, "Visualizing spatial multivalued data," *IEEE Computer Graphics and Applications*, vol. 25, no. 3, pp. 69–79, 2005.
- [34] J. Kehrer and H. Hauser, "Visualization and visual analysis of multifaceted scientific data: A survey," *IEEE Trans. on Visualization and Computer Graphics*, vol. 19, no. 3, pp. 495–513, 2013.
- [35] H. Obermaier and K. I. Joy, "Future challenges for ensemble visualization," *IEEE Computer Graphics and Applications*, vol. 34, no. 3, pp. 8–11, 2014.
- [36] T. Gneiting and A. E. Raftery, "Weather forecasting with ensemble methods," *Science*, vol. 310, no. 5746, pp. 248–249, 2005.
- [37] J. Poco, A. Dasgupta, Y. Wei, W. Hargrove, C. R. Schwalm, D. N. Huntzinger, R. Cook, E. Bertini, and C. T. Silva, "Visual reconciliation of alternative similarity spaces in climate modeling," *IEEE Trans. on Vis. and Comp. Graphics*, vol. 20, no. 12, pp. 1923–1932, 2014.
- [38] U. D. Bordoloi, D. L. Kao, and H.-W. Shen, "Visualization techniques for spatial probability density function data," *Data Science Journal*, vol. 3, pp. 153–162, 2004.
- [39] H. Yan, Y. Qian, G. Lin, L. Leung, B. Yang, and Q. Fu, "Parametric sensitivity and calibration for the kain-fritsch convective parameterization scheme in the wrf model," *Climate Research*, vol. 59, no. 2, pp. 135–147, 2014.
- [40] A. Biswas, G. Lin, X. Liu, and H.-W. Shen, "Visualization of time-varying weather ensembles across multiple resolutions," *IEEE Trans. on Vis. and Comp. Graphics*, vol. 23, no. 1, pp. 841–850, 2017.
- [41] D. Hamby, "A review of techniques for parameter sensitivity analysis of environmental models," *Environmental monitoring and assessment*, vol. 32, no. 2, pp. 135–154, 1994.
- [42] "National hurricane center, uncertainty cone," <http://www.nhc.noaa.gov/aboutcone.shtml>, accessed: 2017-02-05.
- [43] J. Sanyal, S. Zhang, J. Dyer, A. Mercer, P. Amburn, and R. J. Moorhead, "Noodles: A tool for visualization of numerical weather model ensemble uncertainty," *Visualization and Computer Graphics, IEEE Transactions on*, vol. 16, no. 6, pp. 1421–1430, 2010.
- [44] T. Nocke, M. Flechsig, and U. Bohm, "Visual exploration and evaluation of climate-related simulation data," in *2007 Winter Simulation Conference*. IEEE, 2007, pp. 703–711.
- [45] K. Potter, A. Wilson, P.-T. Bremer, D. Williams, C. Doutriaux, V. Pascucci, and C. Johnson, "Visualization of uncertainty and ensemble data: Exploration of climate modeling and weather forecast data with integrated visus-cdat systems," in *Journal of Physics: Conference Series*, vol. 180, no. 1. IOP Publishing, 2009, p. 012089.
- [46] A. Bock, A. Pembroke, M. L. Mays, L. Rastaetter, T. Ropinski, and A. Ynnerman, "Visual verification of space weather ensemble simulations," in *IEEE Scientific Visualization Conference (SciVis)*, 2015, pp. 17–24.
- [47] M. N. Phadke, L. Pinto, O. Alabi, J. Harter, R. M. Taylor II, X. Wu, H. Petersen, S. A. Bass, and C. G. Healey, "Exploring ensemble visualization," in *IS&T/SPIE Electronic Imaging*. International Society for Optics and Photonics, 2012, pp. 82940B–82940B.
- [48] T. Höllt, A. Magdy, G. Chen, G. Gopalakrishnan, I. Hoteit, C. D. Hansen, and M. Hadwiger, "Visual analysis of uncertainties in ocean forecasts for planning and operation of off-shore structures," in *2013 IEEE Pacific Visualization Symposium*, pp. 185–192.
- [49] M. Hummel, H. Obermaier, C. Garth, and K. I. Joy, "Comparative visual analysis of lagrangian transport in cfd ensembles," *IEEE*

- Trans. on Vis. and Comp. Graphics*, vol. 19, no. 12, pp. 2743–2752, 2013.
- [50] J. Cox, D. House, and M. Lindell, “Visualizing uncertainty in predicted hurricane tracks,” *International Journal for Uncertainty Quantification*, vol. 3, no. 2, pp. 143–156, 2013.
- [51] M. Hlawatsch, P. Leube, W. Nowak, and D. Weiskopf, “Flow radar glyphs-static visualization of unsteady flow with uncertainty,” *IEEE Transactions on Visualization and Computer Graphics*, vol. 17, no. 12, pp. 1949–1958, 2011.
- [52] L. Liu, M. Mirzargar, R. M. Kirby, R. Whitaker, and D. H. House, “Visualizing time-specific hurricane predictions, with uncertainty, from storm path ensembles,” in *Computer Graphics Forum*, vol. 34, no. 3. Wiley Online Library, 2015, pp. 371–380.
- [53] K. Matković, D. Gračanin, M. Jelović, A. Ammer, A. Lez, and H. Hauser, “Interactive visual analysis of multiple simulation runs using the simulation model view: Understanding and tuning of an electronic unit injector,” *IEEE Trans. on Visualization and Computer Graphics*, vol. 16, no. 6, pp. 1449–1457, 2010.
- [54] K. Matković, D. Gračanin, R. Splechtna, and H. Hauser, “Interactive visual analysis of families of surfaces: An application to car race and car setup,” in *International Symposium on Visual Analytics Science and Technology*, 2010, pp. 1–7.
- [55] J. Wang, M. Elshehaly, and Y. Cao, “Cylindrical acceleration structures for large hexahedral volume visualization,” in *Large Data Analysis and Visualization (LDAV), 2015 IEEE 5th Symposium on*. IEEE, 2015, pp. 25–31.
- [56] “Scientific visualization contest 2016,” <http://www.uni-kl.de/scviscontest/>, accessed: 2017-01-17.
- [57] A. T. Wilson and K. C. Potter, “Toward visual analysis of ensemble data sets,” in *Proceedings of the 2009 Workshop on Ultrascale Visualization*. ACM, 2009, pp. 48–53.
- [58] E. Sakhaei and A. Entezari, “A statistical direct volume rendering framework for visualization of uncertain data,” *IEEE Trans. on Vis. and Comp. Graphics*, vol. 23, no. 12, pp. 2509–2520, 2017.
- [59] S. Djurcikov, K. Kim, P. Lermusiaux, and A. Pang, “Visualizing scalar volumetric data with uncertainty,” *Computers & Graphics*, vol. 26, no. 2, pp. 239–248, 2002.
- [60] W. Javed and N. Elmquist, “Exploring the design space of composite visualization,” in *Pacific Visualization Symposium (PacificVis), 2012 IEEE*. IEEE, 2012, pp. 1–8.
- [61] G. R. Christie, D. P. Bullivant, S. A. Blackett, and P. J. Hunter, “Modelling and visualising the heart,” *Computing and Visualization in Science*, vol. 4, no. 4, pp. 227–235, 2002.
- [62] J. Kehrer, P. Muigg, H. Doleisch, and H. Hauser, “Interactive visual analysis of heterogeneous scientific data across an interface,” *IEEE Transactions on Visualization and Computer Graphics*, vol. 17, no. 7, pp. 934–946, 2011.
- [63] M. Jarema, I. Demir, J. Kehrer, and R. Westermann, “Comparative visual analysis of vector field ensembles,” in *Visual Analytics Science and Technology, 2015 IEEE Conference on*, pp. 81–88.
- [64] H. Chen, S. Zhang, W. Chen, H. Mei, J. Zhang, A. Mercer, R. Liang, and H. Qu, “Uncertainty-aware multidimensional ensemble data visualization and exploration,” *IEEE Trans. on Vis. and Comp. Graphics*, vol. 21, no. 9, pp. 1072–1086, 2015.
- [65] M. Raj, M. Mirzargar, J. S. Preston, R. M. Kirby, and R. T. Whitaker, “Evaluating shape alignment via ensemble visualization,” *IEEE computer graphics and applications*, vol. 36, no. 3, pp. 60–71, 2016.
- [66] T. Pfaffelmoser and R. Westermann, “Visualizing contour distributions in 2d ensemble data,” *EuroVis-Short Papers*, pp. 55–59, 2013.
- [67] K. Lu, H.-W. Shen, and T. Peterka, “Scalable computation of stream surfaces on large scale vector fields,” in *Proceedings of the International Conference for High Performance Computing, Networking, Storage and Analysis*. IEEE Press, 2014, pp. 1008–1019.
- [68] K. Pöthkow and H.-C. Hege, “Positional uncertainty of iso-contours: Condition analysis and probabilistic measures,” *IEEE Transactions on Visualization and Computer Graphics*, vol. 17, no. 10, pp. 1393–1406, 2011.
- [69] K. Pöthkow and H.-C. Hege, “Nonparametric models for uncertainty visualization,” in *Computer Graphics Forum*, vol. 32, no. 3pt2, 2013, pp. 131–140.
- [70] T. Athawale, E. Sakhaei, and A. Entezari, “Isosurface visualization of data with nonparametric models for uncertainty,” *IEEE transactions on visualization and computer graphics*, vol. 22, no. 1, pp. 777–786, 2016.
- [71] T. Athawale and A. Entezari, “Uncertainty quantification in linear interpolation for isosurface extraction,” *IEEE Trans. on Visualization and Computer Graphics*, vol. 19, no. 12, pp. 2723–2732, 2013.
- [72] T. Pfaffelmoser, M. Reitinger, and R. Westermann, “Visualizing the positional and geometrical variability of isosurfaces in uncertain scalar fields,” in *Computer Graphics Forum*, vol. 30, no. 3, 2011, pp. 951–960.
- [73] O. S. Alabi, X. Wu, J. M. Harter, M. Phadke, L. Pinto, H. Petersen, S. Bass, M. Keifer, S. Zhong, C. Healey *et al.*, “Comparative visualization of ensembles using ensemble surface slicing,” in *IS&T/SPIE Electronic Imaging*. International Society for Optics and Photonics, 2012, pp. 82940U–82940U.
- [74] I. Demir, J. Kehrer, and R. Westermann, “Screen-space silhouettes for visualizing ensembles of 3d isosurfaces,” in *Pacific Visualization Symposium (PacificVis), 2016 IEEE*. IEEE, 2016, pp. 204–208.
- [75] W. He, X. Liu, H.-W. Shen, S. M. Collis, and J. J. Helmus, “Range likelihood tree: A compact and effective representation for visual exploration of uncertain data sets,” in *Pacific Visualization Symposium (PacificVis), 2017 IEEE*. IEEE, 2017, pp. 151–160.
- [76] J. Kniss, S. Premoze, M. Ikits, A. Lefohn, C. Hansen, and E. Praun, “Gaussian transfer functions for multi-field volume visualization,” in *Proceedings of the 14th IEEE Visualization 2003 (VIS'03)*. IEEE Computer Society, 2003, p. 65.
- [77] S. Hazarika, S. Dutta, and H.-W. Shen, “Visualizing the variations of ensemble of isosurfaces,” in *Pacific Visualization Symposium (PacificVis), 2016 IEEE*. IEEE, 2016, pp. 209–213.
- [78] I. Demir, C. Dick, and R. Westermann, “Multi-charts for comparative 3d ensemble visualization,” *IEEE transactions on visualization and computer graphics*, vol. 20, no. 12, pp. 2694–2703, 2014.
- [79] M. Gleicher, D. Albers, R. Walker, I. Jusufi, C. D. Hansen, and J. C. Roberts, “Visual comparison for information visualization,” *Information Visualization*, vol. 10, no. 4, pp. 289–309, 2011.
- [80] V. Verma and A. Pang, “Comparative flow visualization,” *IEEE Transactions on Visualization and Computer Graphics*, vol. 10, no. 6, pp. 609–624, 2004.
- [81] R. Liu, H. Guo, J. Zhang, and X. Yuan, “Comparative visualization of vector field ensembles based on longest common subsequence,” in *IEEE Pacific Visualization Symposium*, 2016, pp. 96–103.
- [82] R. Splechtna, K. Matković, D. Gračanin, M. Jelović, and H. Hauser, “Interactive visual steering of hierarchical simulation ensembles,” in *Visual Analytics Science and Technology (VAST), 2015 IEEE Conference on*. IEEE, 2015, pp. 89–96.
- [83] A. Kumpf, B. Tost, M. Baumgart, M. Riemer, R. Westermann, and M. Rautenhaus, “Visualizing confidence in cluster-based ensemble weather forecast analyses,” *IEEE Transactions on Visualization and Computer Graphics*, vol. 24, no. 1, pp. 109–119, Jan 2018.
- [84] C. M. Bishop, *Pattern recognition and machine learning*. Springer, 2006.
- [85] K. Potter, J. Kniss, R. Riesenfeld, and C. R. Johnson, “Visualizing summary statistics and uncertainty,” in *Computer Graphics Forum*, vol. 29, no. 3. Wiley Online Library, 2010, pp. 823–832.
- [86] M. Ester, H.-P. Kriegel, J. Sander, X. Xu *et al.*, “A density-based algorithm for discovering clusters in large spatial databases with noise.” in *Kdd*, vol. 96, no. 34, 1996, pp. 226–231.
- [87] Z. Wang, A. C. Bovik, H. R. Sheikh, and E. P. Simoncelli, “Image quality assessment: from error visibility to structural similarity,” *IEEE trans. on image processing*, vol. 13, no. 4, pp. 600–612, 2004.
- [88] P. Senin, “Dynamic time warping algorithm review,” *Information and Computer Science Department University of Hawaii at Manoa Honolulu, USA*, pp. 1–23, 2008.
- [89] S.-H. Cha, “Comprehensive survey on distance/similarity measures between probability density functions,” *City*, vol. 1, no. 2, p. 1, 2007.
- [90] P. C. Mahalanobis, “On the generalised distance in statistics,” *Proceedings of the National Institute of Sciences of India*, 1936, pp. 49–55, 1936.
- [91] W. Stuetzle, “Estimating the cluster tree of a density by analyzing the minimal spanning tree of a sample,” *Journal of classification*, vol. 20, no. 1, pp. 025–047, 2003.
- [92] L. Gosink, K. Bensema, T. Pulsipher, H. Obermaier, M. Henry, H. Childs, and K. I. Joy, “Characterizing and visualizing predictive uncertainty in numerical ensembles through bayesian model averaging,” *IEEE transactions on visualization and computer graphics*, vol. 19, no. 12, pp. 2703–2712, 2013.

- [93] R. Kosara, F. Bendix, and H. Hauser, "Parallel sets: Interactive exploration and visual analysis of categorical data," *IEEE Trans. on Vis. and Comp. Graphics*, vol. 12, no. 4, pp. 558–568, 2006.
- [94] J. C. Hunt, A. A. Wray, and P. Moin, "Eddies, streams, and convergence zones in turbulent flows," *Center for Turbulence Research Report CTR-S88, Center for turbulence research, Standford University*, 1988.
- [95] J. Jeong and F. Hussain, "On the identification of a vortex," *Journal of fluid mechanics*, vol. 285, pp. 69–94, 1995.
- [96] M. Otto, T. Germer, H.-C. Hege, and H. Theisel, "Uncertain 2d vector field topology," in *Computer Graphics Forum*, vol. 29, no. 2. Wiley Online Library, 2010, pp. 347–356.
- [97] M. Otto, T. Germer, and H. Theisel, "Uncertain topology of 3d vector fields," in *2011 IEEE Pacific Visualization Symposium*, 2011, pp. 67–74.
- [98] M. Sedlmair, C. Heinzel, S. Bruckner, H. Piringer, and T. Möller, "Visual parameter space analysis: A conceptual framework," *IEEE Transactions on Visualization and Computer Graphics*, vol. 20, no. 12, pp. 2161–2170, 2014.
- [99] D. Coffey, C.-L. Lin, A. G. Erdman, and D. F. Keefe, "Design by dragging: An interface for creative forward and inverse design with simulation ensembles," *IEEE transactions on visualization and computer graphics*, vol. 19, no. 12, pp. 2783–2791, 2013.
- [100] D. Günther, J. Salmon, and J. Tierny, "Mandatory critical points of 2d uncertain scalar fields," in *Computer Graphics Forum*, vol. 33, no. 3. Wiley Online Library, 2014, pp. 31–40.
- [101] L. Liu, A. P. Boone, I. T. Ruginski, L. Padilla, M. Hegarty, S. H. Creem-Regehr, W. B. Thompson, C. Yuksel, and D. H. House, "Uncertainty visualization by representative sampling from prediction ensembles," *IEEE transactions on visualization and computer graphics*, vol. 23, no. 9, pp. 2165–2178, 2017.
- [102] F. Jiao, J. M. Phillips, Y. Gur, and C. R. Johnson, "Uncertainty visualization in hardi based on ensembles of odfs," in *Pacific Visualization Symposium, 2012 IEEE*. IEEE, 2012, pp. 193–200.
- [103] T. Höllt, G. Chen, C. D. Hansen, and M. Hadwiger, "Extraction and visual analysis of seismic horizon ensembles," in *Eurographics (Short Papers)*, 2013, pp. 69–72.
- [104] T. Pfaffelmoser, M. Mihai, and R. Westermann, "Visualizing the variability of gradients in uncertain 2d scalar fields," *IEEE transactions on visualization and computer graphics*, vol. 19, no. 11, pp. 1948–1961, 2013.
- [105] D. Kao, J. L. Dungan, and A. Pang, "Visualizing 2d probability distributions from eos satellite image-derived data sets: A case study," in *Visualization, 2001. VIS'01. Proceedings*. IEEE, 2001, pp. 457–589.
- [106] H. Guo, W. He, T. Peterka, H.-W. Shen, S. M. Collis, and J. J. Helmus, "Finite-time lyapunov exponents and lagrangian coherent structures in uncertain unsteady flows," *IEEE Trans. on Vis. and Comp. Graphics*, vol. 22, no. 6, pp. 1672–1682, 2016.
- [107] H. Guo, X. Yuan, J. Huang, and X. Zhu, "Coupled ensemble flow line advection and analysis," *IEEE transactions on visualization and computer graphics*, vol. 19, no. 12, pp. 2733–2742, 2013.
- [108] R. Liu, H. Guo, and X. Yuan, "A bottom-up scheme for user-defined feature comparison in ensemble data," in *SIGGRAPH Asia 2015 Visualization in High Performance Computing*. ACM, 2015, p. 10.
- [109] R. Liu, H. Guo, and X. Yuan, "User-defined feature comparison for vector field ensembles," *Journal of Visualization*, pp. 1–13, 2016.
- [110] K. Bürger, R. Fraedrich, D. Merhof, and R. Westermann, "Instant visitation maps for interactive visualization of uncertain particle trajectories," in *IS&T/SPIE Electronic Imaging*. International Society for Optics and Photonics, 2012, pp. 82940P–82940P.
- [111] M. Kern, T. Hewson, F. Sadlo, R. Westermann, and M. Rautenhaus, "Robust detection and visualization of jet-stream core lines in atmospheric flow," *IEEE Transactions on Visualization and Computer Graphics*, vol. 24, no. 1, pp. 893–902, Jan 2018.
- [112] J. Poco, A. Dasgupta, Y. Wei, W. Hargrove, C. Schwalm, R. Cook, E. Bertini, and C. Silva, "Similarityexplorer: A visual intercomparison tool for multifaceted climate data," in *Computer Graphics Forum*, vol. 33, no. 3, 2014, pp. 341–350.
- [113] M. M. Malik, C. Heinzel, and M. E. Groeller, "Comparative visualization for parameter studies of dataset series," *IEEE Trans. on Vis. and Comp. Graphics*, vol. 16, no. 5, pp. 829–840, 2010.
- [114] T. Pfaffelmoser and R. Westermann, "Correlation visualization for structural uncertainty analysis," *International Journal for Uncertainty Quantification*, vol. 3, no. 2, 2013.
- [115] M. Otto, T. Germer, and H. Theisel, "Closed stream lines in uncertain vector fields," in *Proceedings of the 27th Spring Conference on Computer Graphics*. ACM, 2011, pp. 87–94.
- [116] C. Petz, K. Pöthkow, and H.-C. Hege, "Probabilistic local features in uncertain vector fields with spatial correlation," in *Computer Graphics Forum*, vol. 31, no. 3pt2, 2012, pp. 1045–1054.
- [117] K. Matković, D. Gračanin, R. Splechtna, M. Jelović, B. Stehno, H. Hauser, and W. Purgathofer, "Visual analytics for complex engineering systems: Hybrid visual steering of simulation ensembles," *IEEE trans. on visualization and computer graphics*, vol. 20, no. 12, pp. 1803–1812, 2014.
- [118] K.-C. Wang, K. Lu, T.-H. Wei, N. Shareef, and H.-W. Shen, "Statistical visualization and analysis of large data using a value-based spatial distribution," in *Pacific Visualization Symposium (PacificVis), 2017 IEEE*. IEEE, 2017, pp. 161–170.
- [119] T.-H. Wei, C.-M. Chen, J. Woodring, H. Zhang, and H.-W. Shen, "Efficient distribution-based feature search in multi-field datasets," in *Pacific Visualization Symposium (PacificVis), 2017 IEEE*. IEEE, 2017, pp. 121–130.
- [120] H. Yu, C. Wang, R. W. Grout, J. H. Chen, and K.-L. Ma, "In situ visualization for large-scale combustion simulations," *IEEE computer graphics and applications*, vol. 30, no. 3, pp. 45–57, 2010.



Junpeng Wang is a Ph.D. student in the Department of Computer Science and Engineering at The Ohio State University. He received his B.E. degree in software engineering from Nankai University in 2011, and M.S. degree in computer science from Virginia Tech in 2015. His research interests are mainly in the visualization and analysis of ensemble simulation data, high-dimensional data, and data generated from machine learning models.



Subhashis Hazarika is a Ph.D. student in the Department of Computer Science and Engineering at The Ohio State University. He received his Bachelors degree in Computer Science from the National Institute of Technology, Durgapur, WB, India in 2011. His research interest includes uncertainty analysis and visualization, ensemble visualization and visual analytics of large-scale scientific data.



Cheng Li is a PhD candidate in computer science at The Ohio State University. His research areas include distribution based data analysis, and interactive data manipulation. He received the BS degree from Tsinghua University, and the MS degree from the University of Iowa. He is a student member of the IEEE and ACM.



Han-Wei Shen is a full professor at the Ohio State University. He received his B.S. degree from Department of Computer Science and Information Engineering at National Taiwan University in 1988, the M.S. degree in computer science from the State University of New York at Stony Brook in 1992, and the Ph.D. degree in computer science from the University of Utah in 1998. From 1996 to 1999, he was a research scientist at NASA Ames Research Center in Mountain View California. His primary research interests are scientific visualization and computer graphics. He is a winner of the National Science Foundation's CAREER award and U.S. Department of Energy's Early Career Principal Investigator Award. He also won the Outstanding Teaching award twice in the Department of Computer Science and Engineering at the Ohio State University.